Applied Soft Computing Journal 84 (2019) 105742

Contents lists available at ScienceDirect

Applied Soft Computing Journal

journal homepage: www.elsevier.com/locate/asoc

Preference-based evolutionary multi-objective optimization in ship weather routing

Joanna Szlapczynska [a,*], Rafal Szlapczynski [b]

[a] Faculty of Navigation, Gdynia Maritime University, Poland
[b] Faculty of Ocean Engineering and Ship Technology, Gdansk University of Technology, Poland

ARTICLE INFO

Article history:
Received 17 March 2019
Received in revised form 9 July 2019
Accepted 26 August 2019
Available online 29 August 2019

Keywords:
Ship weather routing
Multi-objective optimization
Decision maker's preferences
Weight intervals
Trade-off

ABSTRACT

In evolutionary multi-objective optimization (EMO) the aim is to find a set of Pareto-optimal solutions. Such approach may be applied to multiple real-life problems, including weather routing (WR) of ships. The route should be optimal in terms of passage time, fuel consumption and safety of crew and cargo while taking into account dynamically changing weather conditions. Additionally it must not violate any navigational constraints (neither static nor dynamic). Since the resulting non-dominated solutions might be numerous, some user support must be provided to enable the decision maker (DM) selecting a single "best" solution. Commonly, multi-criteria decision making methods (MCDM) are utilized to achieve this goal with DM's preferences defined a posteriori. Another approach is to apply DM's preferences into the very process of finding Pareto-optimal solutions, which is referred to as preference-based EMO. Here the Pareto-set is limited to those solutions, which are compliant with the pre-configured user preferences. The paper presents a new tradeoff-based EMO approach utilizing configurable weight intervals assigned to all objectives. The proposed method has been applied to ship WR problem and compared with a popular reference point method: r-dominance. Presented results prove applicability and competitiveness of the proposed method to solving multi-objective WR problem.

1. Introduction

Multi-objective optimization methods are able to solve variety of real-life optimization problems defined in various technological fields. Nowadays Pareto-optimization methods based on meta-heuristic approach Multi-Objective Meta-Heuristics (MOMH) are especially often utilized [1–5]. This is mostly due to their relatively short computation time and satisfactory level of a true Pareto-front approximation. Among them evolutionary multi-objective optimization (EMO) methods have been gaining increasing attention for the last two decades. In a typical EMO application one aims at optimizing up to three criteria (in case of more than three criteria we talk about many-objective optimization instead) that may be additionally constrained. Since the resulting non-dominated Pareto set is usually numerous, some kind of support is required to select a single solution, "the best" from the decision maker's (DM's) point of view. Commonly, multi-criteria decision making methods (MCDM), such as e.g. ranking methods, are utilized to achieve this goal. When a typical, basic EMO process is completed, the user defines his preferences towards optimization criteria and the ranking method sorts the Pareto-set, thus presenting the best solution on the top of the list.

The majority of real-life multi-objective problems suffer from having large objective space, which results in time consuming optimization process, even when the MOMH/EMO approach is applied. This in turn encourages researchers to propose and develop methods that incorporate DM's preferences into the core of the optimization process to reduce the objective space and thus speed up the convergence of the optimization method. Undoubtedly, there is abundance of works available on preference-based or trade-off approach to EMO, as presented in Section 2.2. The authors of this paper propose here a new preference-based method using configurable weight intervals. The method is then applied to solve ship weather routing multi-objective optimization problem. The problem belongs to a class of constrained multi-objective problems with large objective space, and thus the EMO can greatly benefit from the limitation of the objective space based on DM's preferences.

To properly describe the optimization problem, first some assumptions should be outlined. When a cross-ocean ship voyage is planned, apart from obvious navigational obstacles as landmasses or shallow waters, one also ought to take into account expected wave and wind conditions en route [6]. A storm-tossed ship may finish her voyage with a delay and/or economic loss (e.g. due

* Corresponding author.
E-mail address: j.szlapczynska@wn.umg.edu.pl (J. Szlapczynska).

https://doi.org/10.1016/j.asoc.2019.105742

to damaged commodities), but, what is even more important, could put human life at risk. This is the reason why optimization process in contemporary ship voyage planning systems involves also predicted weather conditions. In literature such approach is usually referred to as weather routing (WR). In WR there is a pursuit to find a route representing a proper balance between economical and safety-related goals. However, one has to bear in mind that WR usually does include ship-to-ship collision avoidance handling, as addressed by a multitude of other papers with [7–9] among others. This paper aims at portraying the application of the hereby proposed preference-based EMO with weight intervals to weather routing optimization problem. The approach presented here could be beneficial to the end users interested in obtaining the balance between various objectives.

The rest of the paper is organized as follows: Section 2 presents a review of works related to the background and core of the problem (weather routing) as well as methods applicable to solve the optimization problem being described (preference-based EMO). Section 3 provides description of the hereby proposed preference-based EMO method with weight intervals together with a detailed description of the optimization problem and EMO framework applied to solve the problem. Then in the following section two example scenarios are presented, showing how application of the proposed method can contribute to the problem being solved. In Section 5 a comparison of the proposed method with a reference point-based one (r-dominance) is presented. Finally, in Section 6 the research results are concluded and future plans are depicted.

2. Related works

The paper addresses problems belonging to two quite distinctive areas: maritime transportation (ship weather routing) and preference-based evolutionary multi-objective optimization (EMO). Thus, in the following subsections separate literature reviews on these two topics have been provided.

2.1. Weather routing of ocean-going vessels

The first weather routing approach was the isochrone method [10], proposed for manual use and based on geometrically determined and recursively defined time fronts (isochrones). In the next decades computer implementations of the method were developed, as presented in [11], among others. The isochrone method utilizes single-objective approach (usually for passage time minimization) and has limited possibility of handling dynamic constraints. Direct application of the original isochrone method to a computer algorithm may result in having so-called "isochrone loops". Despite its limitations the isochrones method is still popular and there are some up-to-date commercial weather routing systems that still utilize it, albeit in a highly modified fashion.

There are also multiple other approaches to the weather routing problem. Basic use of dynamic programming for a grid of points has been proposed in [12,13]. Also 3D dynamic programming approaches to weather routing are applied [14,15]. As presented in [16], solving specified optimal control problem allows for finding time-optimal path. Another approach using Dijkstra algorithm was presented in [17,18] and in [19,20].

All the above-mentioned methods utilize single-objective optimization, usually focused on passage time or fuel consumption minimization. A multiobjective approach to ship route planning has been proposed in [21], however the objectives were aggregated there to a single criterion. Purely mathematical approach to such optimization with Pareto-optimal sets of solutions has been initially proposed in [22–26]. The methods in [23,24] utilize MOGA algorithms. In the works by [22,25,26] the more robust SPEA/SPEA2, multi-objective evolutionary approach has been applied.

2.2. Preference-based Evolutionary Multi-objective Optimization (EMO)

A popular trend in Multi-Objective Meta-Heuristics (MOMH) is to take into account decision-maker's (DM) preferences. This allows the algorithm to focus on the part of the objective space, which is most interesting to DM. Among others, limiting the objective space makes it possible to reduce Pareto front and thus speed up the convergence to the final representation of a Pareto-optimal set. Making use of DM's preferences can be done in a number of ways [27]. The dominating one is that of a reference point (RP) — a point in the objective space, which represents a solution that is desired and seems possible to be reached [28–30]. An RP may be used for dominance relation [31,32], as well as for crowding distances and sorting non-dominated Pareto sets [33,34]. Similarly, a reference direction can be specified [35]. If the DM is unable to specify a single RP, it is also possible to provide a preference region. Reflecting DM's satisfaction with solutions in the preference region may be done by means of desirability function [36,37], density function [38] or a combinations of both [39]. Other approaches to applying DM's preferences include those of objective comparison [40], solution comparison [41], outranking [42,43], knee points [27,44] and trade-offs [33,45–47]. Of those, trade-off approach is the most natural for weather routing purposes, where a DM is interested in a configurable balance between economic and safety-related objectives.

Trade-off can be classified as objective (based on the structure of the problem) or subjective (reflecting DM's arbitrary preferences). Subjective trade-off may take as input data linguistic terms [48] (which can then be converted to weight intervals) or coefficients. Subjective trade-off approach utilizing DM-specified trade-off coefficients has been introduced in [45] where it has been applied in a guided multi-objective evolutionary algorithm. The subjective trade-off proposed there reflects how much the DM is ready to sacrifice the value of some objectives in order to improve other. Trade-off can be given in units:. DM may state that a single unit improvement in one objective is worth at most n units degradation in another objective.

Such approach works very well for bi-objective optimization but, as has been observed in [27] the authors of [45] have not extended their approach to more than two objectives. This transition to a larger number of objectives is done in the current paper.

For any given number of objectives subjective trade-off can be implemented as a matrix of trade-off coefficients, where each coefficient $c_{i,j}$ reflects the degradation in jth objective, that a DM is willing to accept in order to gain a 1 unit improvement in the ith objective. However, such matrix of coefficients is impractical in direct use for two reasons:

- it is inconvenient to apply it in dominance rules for more than two objectives,
- DM can enter inconsistent values, so a consistency check has to made afterwards and DM should correct coefficient values if necessary.

Fortunately, both problems can be eliminated if instead of coefficients we decide to operate on weight intervals assigned to each objective.

3. Proposed preference-based evolutionary multi-objective optimization

The method proposed here, despite nominal similarity to weight-based approaches [38,46] can actually be classified as a modified subjective trade-off approach, which extends the concept of [45] from bi-objective to multi-objective. If needed, it can also be extended so as to take DM's input parameters in the form of linguistic terms, which can later be converted to weight intervals (as shown in [48]).

3.1. Trade-off by means of weight intervals

Let us denote a DM-given interval of weights assigned to the ith objective as:

$$w_i \in \left\langle w_i^{\min}, w_i^{\max} \right\rangle, \tag{1}$$

where $w_i^{\min}, \in \langle 0, 1\rangle$, $w_i^{\max} \in (0,\ 1\rangle$ and $w_i^{\min} \le w_i^{\max}$.

Based on (1), throughout the paper a generalized weighted average objective function will be used:

$$f(x) = \sum_{i=1}^{n} w_i f_i(x), \tag{2}$$

where n is the number of objectives and each $f_i(x)$ is a normalized objective function which returns values from $\langle 0, 1\rangle$ range. It must be noted here, that each w_i remains an unspecified value from the $\left\langle w_i^{\min}, w_i^{\max} \right\rangle$ range. Therefore $\sum_{i=1}^{n} w_i$ is not always equal to one. Instead, it can be any number between zero and n. As for objective functions $f_i(x)$, it is assumed that their values are condensed down to $\langle 0, 1\rangle$ range prior to evolutionary operations (including dominance check). It is essential to use normalized objective functions because otherwise the weight intervals would not truly reflect DM's preferences: the objective function of the largest range would have the largest impact on the dominance rules and on the multi-criteria decision making phase. Therefore, in practice it is recommended to normalize objective functions values "on the way" — during each generation of the evolutionary algorithm. It is also important to minimize the loss of information caused by the normalization (Min–Max Feature Scaling may be undesired as it always covers the full $\langle 0, 1\rangle$ range, even if pre-normalized values are close to each other).

For the generalized weighted average function from (2), the following always holds:

$$\sum_{i=1}^{n} w_i^{\min} f_i(x) \le f(x) \le \sum_{i=1}^{n} w_i^{\max} f_i(x). \tag{3}$$

In Pareto multi-objective minimization x dominates y if and only if:

$$\exists_i \left(f_i(x) < f_i(y)\right) \ \text{ and } \forall_i \left(f_i(x) \le f_i(y)\right). \tag{4}$$

For the proposed generalized weighted average objective function the above rule still holds in the sense that it implies dominance. However, if the rule (4) is not satisfied and x does not dominate y, the extended relation of weight interval-based dominance might be used instead of Pareto dominance by checking a condition:

$$f(x) < f(y), \tag{5}$$

where $f()$ is the generalized weighted average function given by (2).

Checking whether (5) holds true cannot be done directly, because each w_i remains an unspecified value from $\left\langle w_i^{\min}, w_i^{\max} \right\rangle$ range. However, it can be shown that (5) is always true if the following holds true:

$$\sum_{i=1}^{n} g_i(x, y) > 0, \tag{6}$$

where:

$$g_i(x, y) = \begin{cases} w_i^{\min} \left(f_i(y) - f_i(x)\right), & \text{for } f_i(y) - f_i(x) \ge 0 \\ w_i^{\max} \left(f_i(y) - f_i(x)\right), & \text{for } f_i(y) - f_i(x) < 0, \end{cases} \tag{7}$$

The above described preference-based method is summarized in Fig. 1.

3.2. Optimization problem in weather routing

When predicted weather conditions are considered in ship routing, the optimization problem should be defined as multi-objective weather routing. In general, there are two groups of goals to be satisfied in the routing, namely economical and safety-related ones. Thus, following the past research by one of the authors [49], a route is defined as a vector of controlpoints from the point of departure to the destination. Two route's consecutive controlpoints define a leg. Each controlpoint stores information of its location (latitude and longitude), time of arrival (based mainly on past legs, forecasted weather conditions in its vicinity and ship's speed characteristics) and a number of additional leg-related parameters (e.g. engine settings, ship course, etc.). Route's optimization criteria set includes minimization of passage time and fuel consumption while assuring the highest possible voyage safety, as presented by (8)–(10), respectively:

$$f_{passage\_time}() \rightarrow \min, \tag{8}$$

$$f_{fuel\_consumption}() \rightarrow \min, \tag{9}$$

$$f_{safety\_index}() \rightarrow \max. \tag{10}$$

Values of the goal functions (8)–(10) are computed for considered routes for the assumed ship model: a double decker general dry cargo vessel, described in detail in [50]. Route's passage time is computed based on the ship model's speed characteristics (which usually take form of plots with predicted ship speed for wave and/or wind encounter angles, loading conditions, etc.) and forecasted weather data (including speed loss on waves) for each consecutive route's controlpoint. Thus, a total route's passage time given by (8) in hours is a sum of all passage times required to go through all route's legs. The computed passage time for a route depends strongly on weather conditions forecasted for its controlpoints. Thus, locations (lat; lon) of the controlpoints are the key variables contributing to passage time computation. However, weather conditions are not static (in time domain), so reaching a given location at different moments in time can lead to completely different weather conditions encountered and thus further affect passage time. Indeed, dynamic nature of weather conditions (which affect both WR criteria and constraints) is what makes the optimization problem in weather routing quite challenging.

As for fuel consumption, it is computed based on the ship model engine settings (leg-related), engine power on still water (assumed constant for given ship model and loading conditions) and power loss due to waves (based on ship model and forecasted weather conditions). Again, a total route's fuel consumption given by (9) in tons is a sum of fuel consumed at each route's leg. As in the previous case, this criterion depends on dynamic nature of forecasted wave conditions (significant wave height and wave direction are taken into account) and location of the controlpoints.

Safety index for a route's leg is a normalized value (in <0.0; 1.0> range) computed based on ship model stability calculus. Minimal fractional index (computed for each controlpoint) with value 0.0 depicts fully unsafe situation, whereas maximal value 1.0 depicts that the ship is hypothetically absolutely safe. The index is computed by taking forecasted weather conditions valid for the leg as inputs. Unlike the previous goal functions, total safety index (dimensionless) for a route given by (10) is computed as an average of the fractional safety indices over all route's legs. To handle rare but extreme weather conditions (increasing the average only slightly) additional optimization constraints have been added.

The optimization constraint set in WR includes:

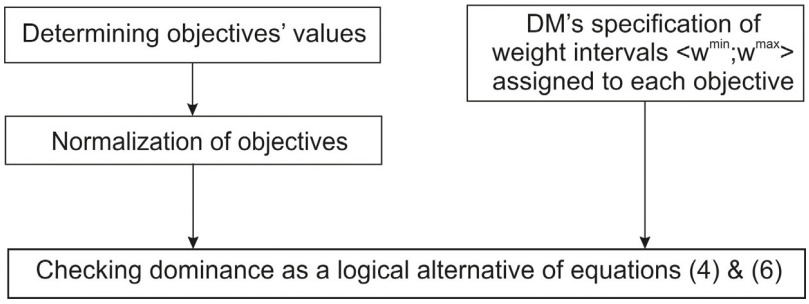

Fig. 1. Proposed preference-based method.

1. landmasses and shallow waters (for given ship model's draught), which is a compulsory constraint in any ship routing problem — a static constraint, whose data can be read from Electronic Navigational Chart (ENC),
2. wind fields en route with wind speed above given threshold value (here the value is set as 40kn, which reflects sea state between 8 and 9 in Beaufort scale) — a dynamic (varying with time) constraint,
3. areas with stability-related phenomena according to IMO Circ. #1228 as described in [51] — a dynamic constraint.

Checking if the first two constraints are met is relatively simple. The third one, however, is more complex. Three types of stability-related phenomena are handled here:

- resonance — (including synchronous and parametric rolling motions) occurs when natural ship rolling is equal to encounter wave period or its doubled value, may result with high amplitude heavy ship oscillations,
- successive high wave attack — occurs when wave length and significant wave height are in certain relation with ship size, may result with large roll angles or capsizing in extreme cases,
- surf-riding and broaching-to — occurs when wave speed is in certain relation with ship size, may result with ship course deviation or capsizing in extreme cases.

Of these, resonance is the most frequent. For every controlpoint each of the stability-related phenomena have to be checked whether a particular combination of a vessel's course and speed with forecasted weather conditions is safe. The constraint can easily make many routes unacceptable and thus it affects the final Pareto set in large degree.

In terms of variable space, the objectives of each route depend on the geographical coordinates (longitude and latitude) of all its controlpoints. The number of controlpoints varies depending on a particular route. Transatlantic routes have the average of about 100 controlpoints, which gives 200 variables. Therefore it can be assumed, that each objective is a function of about 200 variables. Each variable is a real number representing the latitude or longitude from a given range (depending on the predefined start and destination points). As a result, the search space of the optimization problem is large so it is desired to come up with any methods that can speed up the convergence of the optimization process.

When the EMO approach with trade-offs by means of weight intervals (see Section 3.1) is applied to the optimization problem described here, the $w^{\min}$ and $w^{\max}$ values are assigned to each of the optimization criteria given by the goal functions (8)–(10).

3.3. The motivation behind applying the proposed weight interval-based trade-off approach

As mentioned in Section 2.2, the most popular thread in incorporating DM's preferences is the one utilizing reference points (RP). RPs are convenient and effective technique supplementing MOMH in many branches of technical sciences and industry. Their only limitation is that Decision Maker (DM) has to know the RP coordinates. E.g. in optimizing design of mechanical, electrical or electronic devices DM usually knows or suspects that a certain combination of objective values is possible. DM may know this because particular devices are available and the information on their performance can be accessed. However, in case of weather routing little is known about possible objective values until exact solutions are obtained. Some combination of fuel consumption, safety and passage time could have been possible for certain start-destination parameters in the past, but they may no longer be possible in future. Seasonal weather changes (in extreme cases including cyclones, which have to be avoided at all costs), climate changes, particular ship performance parameters (especially speed characteristics), loading etc. all greatly affect navigation conditions. Otherwise, ship-owners and navigators could simply re-use old routes or route patterns, as it used to be a few decades ago, without the up-to-date data-driven weather routing optimization process.

Furthermore, it must be emphasized here, that both ship-owners and navigators may have to run weather routing optimization multiple times for a single journey, especially for a cross-ocean one. Although weather forecast services have advanced in terms of data collection and modelling, the weather changes are now more dynamic than ever, which makes weather predictions harder. The accuracy of those predictions decreases for more distant time horizons and the forecasts for a week ahead are of limited reliability. Therefore, apart from performing weather routing before the journey, it is recommended to repeat this process on the way. In practice, every time a new weather forecast is available, the system should re-run weather routing algorithm starting from the ship's current position. In case of using RP it would involve specifying new RP coordinates at least every 24 h for the remaining part of a route. Apart from being simply inconvenient, it would also be hard feasible. While fuel consumptions and passage times may be archived for whole routes (from departure till arrival) such past data is usually not available for incomplete route parts. Consequently, a navigator would have to enter new RP coordinates periodically without unsupported by any reliable data.

Another important issue is that a ship-owner may be interested in specifying one policy for a whole fleet of various vessels navigating between various start and destination points. The proposed approach to DM's preferences is context-free. It reduces ship-owner's involvement to providing six numbers (assumed having three criteria) only once. If necessary, ship-owner may even input linguistic terms, which can then be automatically converted to weight intervals, as shown in [48]. As opposed to this, any RP-based method would require setting RP coordinates separately for each combination of route endpoints, particular vessel (including its speed characteristics and loading conditions)

and time of the year (because of seasonal weather changes). Even if technically possible, it would be extremely troublesome. The proposed approach greatly saves DM's time while being competitive in terms of approximating Pareto front and supporting multi-criteria decision-making phase of weather routing process.

3.4. MEWRA as a tool for solving the optimization problem in weather routing

Multi-objective Evolutionary Weather Routing Algorithm (MEWRA) is a tool for ship route optimization utilizing Strength Pareto Evolutionary Algorithm 2 as proposed in [52]. MEWRA has been developed by one of the authors to support ship routing decisions. In its current form, it is integrated as a research tool with an ENC-class software NaviWeather by NavSim Poland.

In [22] the first draft of a Multi-objective Evolutionary Weather Routing Algorithm (MEWRA) with continuous-space optimization has been proposed, designed initially for a ship model with hybrid propulsion. A new engine-based MEWRA [51] has been presented in [49] together with customizable criteria and constraints sets. The approach has been further extended towards exclusion of areas with resonance phenomena (surf-riding and broaching to, successive high wave attack and resonance) according to IMO Circ. #1228 [51] and reliable synchronous roll prediction [50].

An evolutionary individual in the algorithm is a route, represented by a vector of controlpoints with associated geographical coordinates (lon & lat) and additional ship-related settings. In general MEWRA comprises of the following elements, depicted in Fig. 2:

- initial population generation,
- core evolutionary optimization (SPEA2), including standard mutation & crossover operators,
- deterministic algorithms extending the evolutionary algorithm (including A* used for pre-optimization route finding in narrow passages),
- multiple problem-dedicated operators,
- multi-criteria ranking method to limit the resulting non-dominated solution set to the element the most suitable from the decision maker's point of view.

Selected elements listed above are briefly described below. As for generating initial population, the population comprises of initial feasible routes (i.e. not violating any of the defined optimization constraint). Generation process is random, but driven by a set of pre-defined routes (between given origin and destination points), such as:

- rhumb line (on map with Mercator projection it is a straight line between origin and destination),
- Great Circle (shortest distance between origin and destination points on the globe, without taking into account weather conditions, ship modelling, bathymetry, etc.),
- a reflected Great Circle (along the rhumb line),
- direct route generated by A* algorithm.

Problem dedicated operators include among others:

- operators responsible for loop removal (unintended loops formed by the subsequent controlpoints),
- operators ensuring that bathymetry-related constraints are met.

The latter assure that the ship's route does not cross land or other obstacles and that ship retains sufficient clearance under keel along the whole route. If a violation of a bathymetric constraint is detected, one of the route-modifying operator may be selected.

Table 1
Evolutionary settings common for Scenario 1 & 2.

Parameter name	Value
Max. number of generations	100
Population size	100 individuals (routes)
Non-dominated set size	100 individuals (routes)
Crossover probability	0.6
Mutation probability	0.4
Optimization criteria	1. passage time → min 2. fuel consumption → min 3. safety of passage → max

The choice of an operator is random, but particular operator may be favoured depending on the length of a route's segment, which violates the constraint and the coordinates of the violating segment's endpoints. The bathymetry-related operators include:

(a) inserting a new segment of a route,
(b) inserting a new controlpoint,
(c) shifting a whole segment of a route ,
(d) shifting a controlpoint of a problematic segment.

All of those operators are shown in Fig. 3. It is worth noting that although random, they are parametrized by the size of constraint violation and violation's relative location within the route's segment. While none of those operators guarantees eliminating a violation, they work very well in the sense that they greatly speed up obtaining acceptable solutions.

4. Validation and verification of the approach — example scenarios

The proposed preference-based EMO, described in details in Section 3.1, has been validated and verified in a series of computer simulations conducted by MEWRA. Two scenarios have been selected with different passages (voyage departure & destination points) and different weather conditions (having direct impact on the optimization process):

- Scenario 1: voyage from Miami to Lisbon in February 2017,
- Scenario 2: voyage from Plymouth to Miami in September 2013.

The first scenario accentuates narrowing down the weight intervals (assumed weight intervals are equal for all criteria) subject to investigating how the interval's width limits the size of Pareto front. Scenario 2 focuses on presenting how the weight intervals could model decision maker's preferences during the core multi-objective optimization. Settings common to both scenarios are presented in Table 1. Probability values for crossover and mutation have been determined in the course of study on weather routing problem [49], thus they differ from standard crossover and mutation probability values as strictly problem-oriented.

NOAA Wave Watch III model has been utilized as a source of weather forecasts for both scenarios. Wind direction and speed parameters are directly forecasted by NOAA Wave Watch III model, while wave conditions (significant wave height, wave period and wave direction) are estimated based on the forecasted wind conditions.

4.1. Scenario 1: voyage from Miami to Lisbon in February 2017

In this scenario a voyage from Miami coastal waters with departure on 25th February 2017 at 00:00 UTC with destination Lisbon has been simulated in MEWRA. A set of three optimization criteria has been considered, namely: passage time (min), fuel consumption (min) and safety of passage (max). Assumed

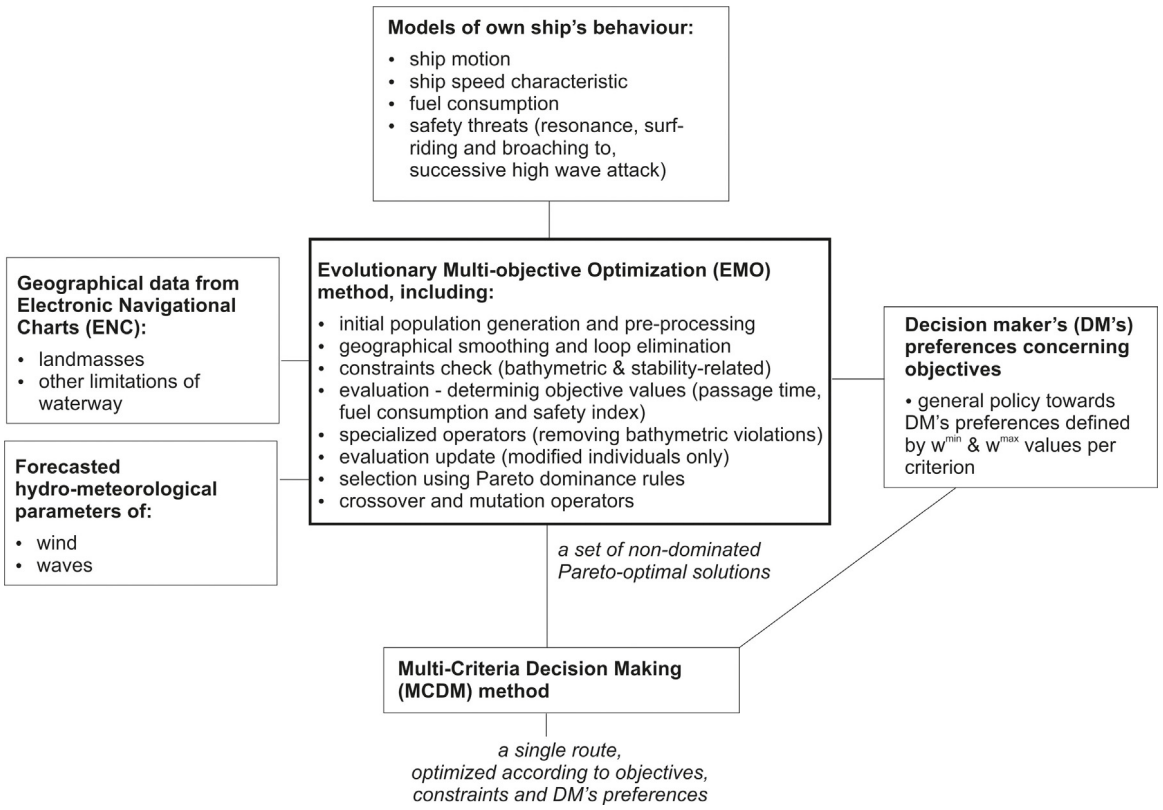

Fig. 2. Overview of the MEWRA optimization tool with proposed preference-based approach.

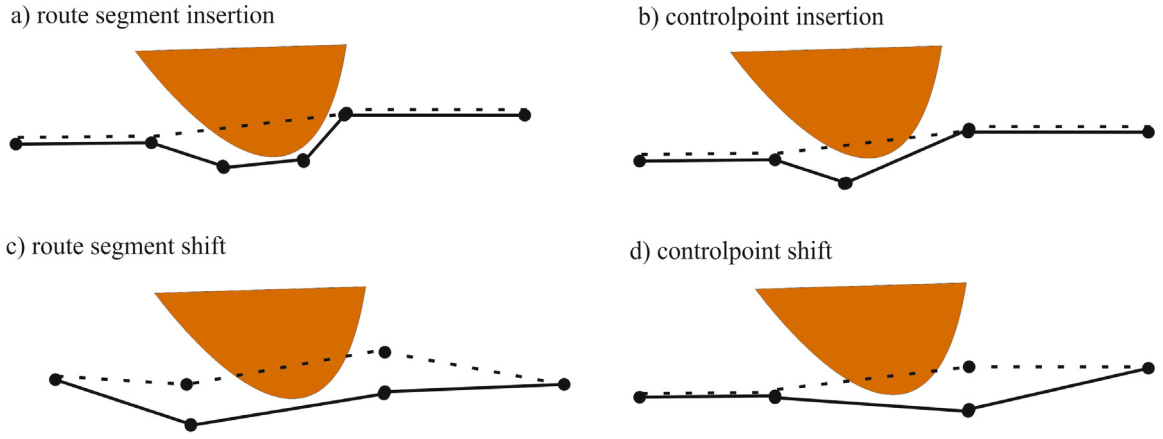

Fig. 3. Examples of problem-dedicated operators, which modify a route.

constraints in the optimization process, apart from obvious landmasses and shallow waters (static), are: wind fields above 40kn (dynamic) and areas with resonance phenomena according to IMO Circ. #1228.

During the planned voyage some strong wind, and consequently wave, fields was forecasted, thus limiting northern Miami–Lisbon passages. Also unfavourable conditions in terms of possible resonance phenomena were predicted in the area of the crossing of 30°N and 50°W through the first 100h after departure. Detailed overview of weather conditions during the voyage (in terms of wind speed and direction) are presented by set of figures provided in Appendix A.

In this scenario three sets (cases) of weight intervals (Table 2) have been simulated for the assumed voyage in order to verify if, and to which extent, narrowing down the weights' width limits the resulting Pareto set. For each case the weight intervals are equal for all the three optimization criteria. Fig. 4 presents resulting Pareto front obtained by utilization of "regular Pareto dominance", here regarded as a reference. Then Figs. 5–7 present Pareto fronts obtained for the same voyage and case no. 1–3, accordingly. In Figs. 8–10 the Pareto fronts (red dots) from Figs. 5–7 are presented in 3D objective function space together with a reference Pareto front from Fig. 4 (blue dots). It is worth noting that the shapes of Pareto fronts are closer to 3D curves than surfaces because two of the optimization objectives (passage time

Table 2
Values of preference-based Pareto dominance weight intervals (w^{min}, w^{max}) assigned in cases 1–3 of Scenario 1.

	Case no.	Passage time		Fuel consumption		Safety of passage	
		w^{min}	w^{max}	w^{min}	w^{max}	w^{min}	w^{max}
Scenario 1	1	0.1	0.9	0.1	0.9	0.1	0.9
	2	0.25	0.75	0.25	0.75	0.25	0.75
	3	0.33	0.66	0.33	0.66	0.33	0.66

Table 3
Average Pareto size of repeated "regular domination" and cases 1–3 of Scenario 1.

		Average Pareto size
Scenario 1	Case 0 ("regular dominance")	62,60
	Case 1 ($w^{min} = 0.1$ and $w^{max} = 0.9$)	4,90
	Case 2 ($w^{min} = 0.25$ and $w^{max} = 0.75$)	2,60
	Case 3 ($w^{min} = 0.33$ and $w^{max} = 0.66$)	1,60

and fuel consumption) are related in case of the selected vessel model.

As presented in Figs. 5–10 the resulting Pareto set of routes, as expected, gets significantly reduced when the preference-based Pareto-dominance is applied. The "regular Pareto dominance" example provided in Fig. 4 has been taken as a reference here. The smaller width of weight interval (w^{max} - w^{min}) the easier it is for one solution to dominate the other, which results in largely reduced non-dominated Pareto set. In the example provided above Pareto size is reduced from 63 routes ("regular domination"), to 6 routes for case 1 ($w^{min} = 0.1$ and $w^{max} = 0.9$), further to 2 routes for case 2 ($w^{min} = 0.25$ and $w^{max} = 0.75$) and finally to just a single route for case 3 ($w^{min} = 0.33$ and $w^{max} = 0.66$).

Obviously, the optimization process may finalize with different result (Pareto size) each time since the evolutionary metaheuristic is able to find only a discrete approximation of the Pareto-optimal set, not the true Pareto-optimal set. Thus, in this scenario the optimization process for each case of weight interval has been repeated (10 repetitions) to verify if the Pareto set reduction level is kept. Table 3 presents average values of the Pareto set size for the "regular domination" and preference-based dominance case 1–3. Tendency of narrowing the Pareto set is clearly indicated by average Pareto size as presented in Table 3 as the size shrinks drastically with decreasing value of weight interval (w^{max} - w^{min}). Obviously, the minimal possible Pareto front size is 1 element (a single route), since always at least one individual would have to remain non-dominated by all the other individuals.

4.2. Scenario 2: voyage Plymouth–Miami in September 2013

In this scenario a voyage from Plymouth coastal waters with departure on 27th September 2013 at 00:00 UTC with destination Miami has been simulated in MEWRA. Similarly to the previous scenario, the following optimization criteria have been considered, namely: passage time (min), fuel consumption (min) and safety of passage (max). As before, the last criterion is represented by safety index mainly based on stability of the ship. Due to forecasted weather conditions for Atlantic Ocean in the considered time-frame (see Fig. A.2) the constraint of resonance phenomena has been excluded in this scenario. Thus, the optimization constraint set consists here of just two elements, namely landmasses and shallow waters (static) and wind fields above 40kn (dynamic).

This scenario aims at discovering to what extent the weight intervals can model decision maker's preferences when weight intervals are applied to the core multi-objective optimization. Thus, apart from the case 0 ("regular Pareto dominance"), the following two cases have been considered here, as presented in Table 4. Case 1 presents situation of strongly preferred time & fuel to safety, whereas case 2 presents the opposite situation.

Fig. 11 presents resulting Pareto front obtained by utilizing "regular Pareto dominance", here regarded also as a reference. Then Figs. 12–13 present Pareto fronts obtained for the same voyage and case no. 1–2, accordingly. In Figs. 14–15 the Pareto fronts (red dots) from Figs. 12–13 are presented in 3D objective function space together with a reference Pareto front from Fig. 11 (blue dots).

Similarly to the previous scenario, simulations for cases 1 and 2 of Scenario 2 have been repeated to validate if the results are reproducible. Based on the sets of results two aggregated 3D Pareto front figures have been prepared: Fig. 16 presenting aggregated case 1 results and Fig. 17 with aggregated case 2 results. In both Figs. 16 and 17 red dots depict aggregated Pareto front elements (obtained by repeated application of MEWRA with weight interval) and blue dots depict the reference Pareto front in Scenario 2 (obtained by application of MEWRA with "regular domination", thus without weight intervals).

In Scenario 2 case 1 weight intervals have been set the way to underline strong decision maker's preferences towards passage time (min) and fuel consumption (min) criteria and opposite to safety of passage (max) criterion. The aggregated Pareto front plot (Fig. 16) reveals that all the resulting non-dominated solutions (red dots) are gathered near left-most elements of the reference Pareto front (blue dots) where routes have small values of both passage time and fuel consumption.

In Scenario 2, case 2 there is an opposite case described. This time the weight intervals reflect strong decision maker's preferences towards maximized safety of passage while paying less attention to economic performance route indices (time & fuel). In Fig. 17 the aggregated non-dominated solutions (red dots) are gathered near the part of the reference Pareto front (blue dots) with the highest safety index value. What is worth noticing is that here some of the red dots are above the blue to with the highest safety index which shows that the preference-based Pareto dominance holds a possibility of the Pareto front extrapolation (obtained simply by a faster convergence) towards given user preferences.

4.3. Conclusions

As presented in Scenario 1 the preference-based Pareto optimization is able to reduce the resulting non-dominated set. The reduction level may be adjusted by narrowing or widening width of weight intervals (w^{min},w^{max}) associated with given optimization criteria. What is more, the solution presented here is also able to map decision maker's preferences onto the resulting non-dominated set of solutions. This may be achieved by assigning weight intervals of greater (closer to 1.0) values of w^{min} and w^{max} to these criteria that are considered more important and smaller w^{min} and w^{max} values (closer to 0.0) to those that are considered less important according to the DM.

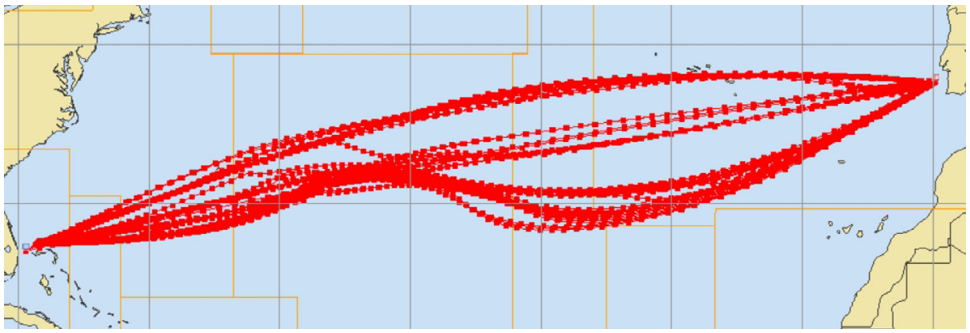

Fig. 4. Miami–Lisbon, departure on 25th February 2017 at 00:00 UTC, Pareto front (63 routes) obtained by MEWRA utilizing "regular Pareto dominance" (Case 0) in Scenario 1.

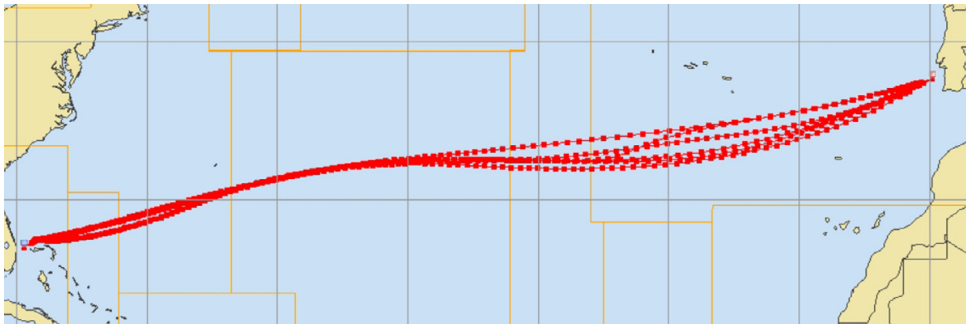

Fig. 5. Miami–Lisbon, departure on 25th February 2017 at 00:00 UTC, Pareto front (6 routes) obtained by MEWRA with weight intervals $w^{\min} = 0.1$ and $w^{\max} = 0.9$ for each criterion (Case 1) in Scenario 1.

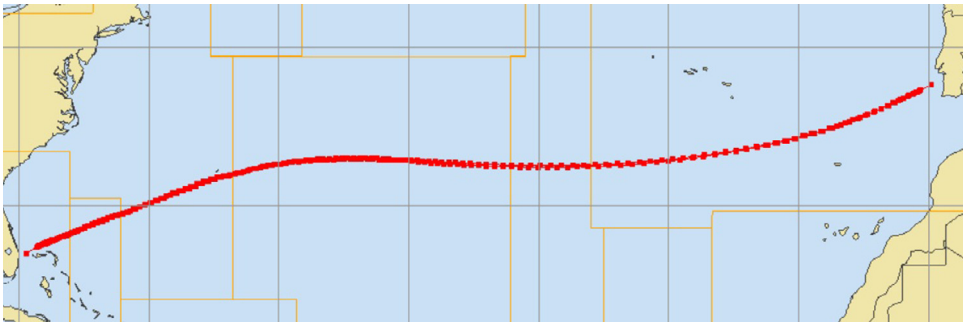

Fig. 6. Miami–Lisbon, departure on 25th February 2017 at 00:00 UTC, Pareto front (2 routes) obtained by MEWRA with weight intervals $w^{\min} = 0.25$ and $w^{\max} = 0.75$ for each criterion (Case 2) in Scenario 1.

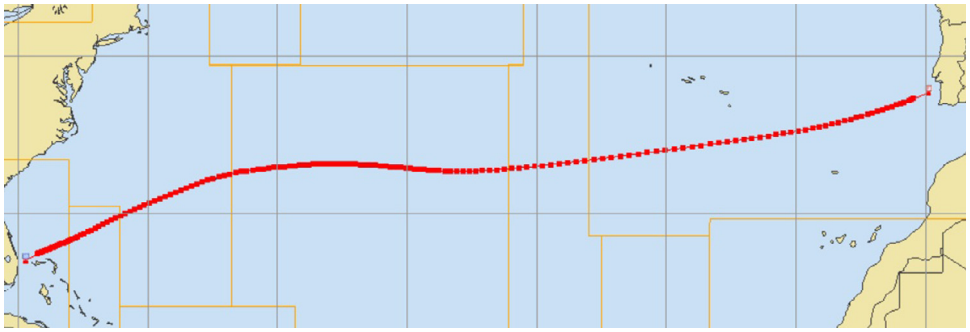

Fig. 7. Miami–Lisbon, departure on 25th February 2017 at 00:00 UTC, Pareto front (1 route) obtained by MEWRA with weight intervals $w^{\min} = 0.33$ and $w^{\max} = 0.66$ for each criterion (Case 3) in Scenario 1.

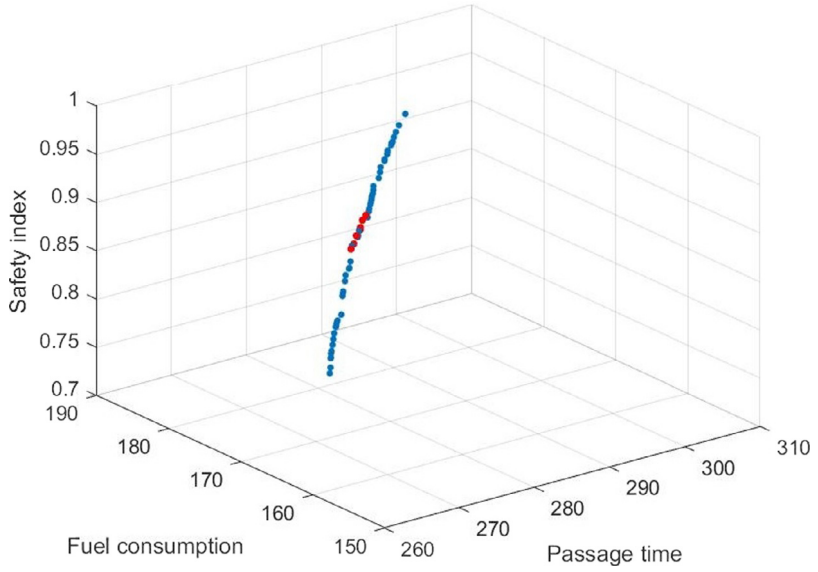

Fig. 8. Miami–Lisbon, departure on 25th February 2017 at 00:00 UTC, Pareto front (6 routes, red dots) in objective function space obtained by MEWRA with weight intervals $w^{\min} = 0.1$ and $w^{\max} = 0.9$ for each criterion (Case 1) with a reference Pareto front obtained by "regular domination" (blue dots) in Scenario 1.

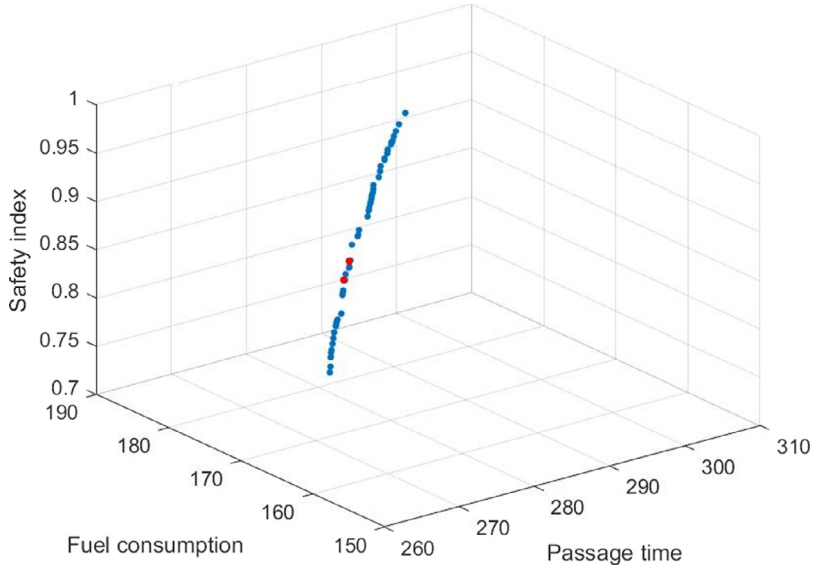

Fig. 9. Miami–Lisbon, departure on 25th February 2017 at 00:00 UTC, Pareto front (2 routes, red dots) in objective function space obtained by MEWRA with weight intervals $w^{\min} = 0.25$ and $w^{\max} = 0.75$ for each criterion (Case 2) with a reference Pareto front obtained by "regular domination" (blue dots) in Scenario 1.

Table 4
Values of preference-based Pareto dominance weight intervals ($w^{\min}$, $w^{\max}$) assigned in cases 1–2 of Scenario 2.

	Case no.	Passage time		Fuel consumption		Safety of passage	
		$w^{\min}$	$w^{\max}$	$w^{\min}$	$w^{\max}$	$w^{\min}$	$w^{\max}$
Scenario 2	1	0.5	1.0	0.5	1.0	0.1	0.5
	2	0.1	0.5	0.1	0.5	0.5	1.0

5. Comparison of the proposed preference-based approach with r-dominance

Below we are presenting a comparison of the proposed approach with a selected RP method, emphasizing the sensitivity of the RP method to the choice of particular RP coordinates. Two possible RP methods have been taken into account initially: r-dominance [31,32] and reference vector. However, it has been decided that while a single RP can be in some cases provided by DM, it would be nearly impossible for to come up with a truly reliable reference vector. Therefore, r-dominance is used throughout the comparison shown in this section.

The key issue in utilization of any reference point-alike method is to properly choose the RP point. Ideally, the RP point should be close to hypothetically the best possible solution, usually located in the Pareto front or in its close vicinity. However, in weather routing it is extremely hard to provide any reasonable RP point in advance, before any optimization starts. It is simply due to

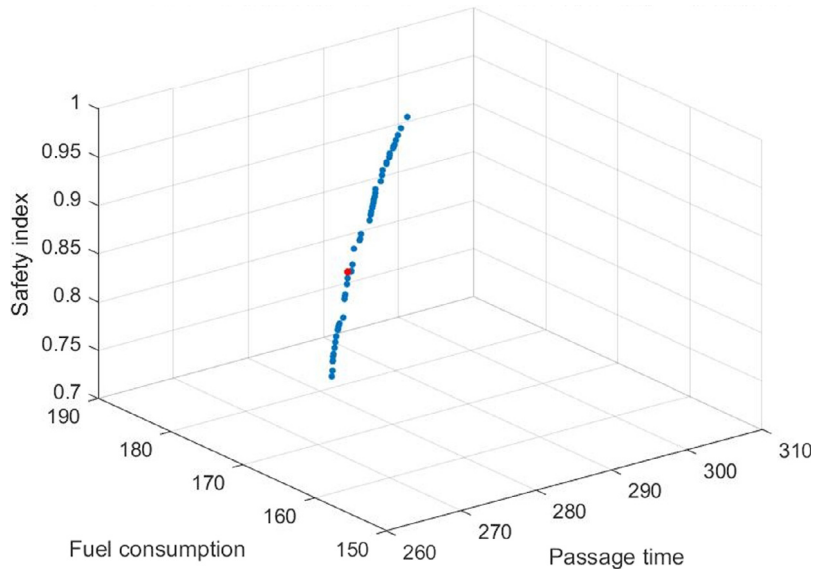

Fig. 10. Miami–Lisbon, departure on 25th February 2017 at 00:00 UTC, Pareto front (1 route, red dot) in objective function space obtained by MEWRA with weight intervals $w^{\min} = 0.33$ and $w^{\max} = 0.66$ for each criterion (Case 3) with a reference Pareto front obtained by "regular domination" (blue dots) in Scenario 1.

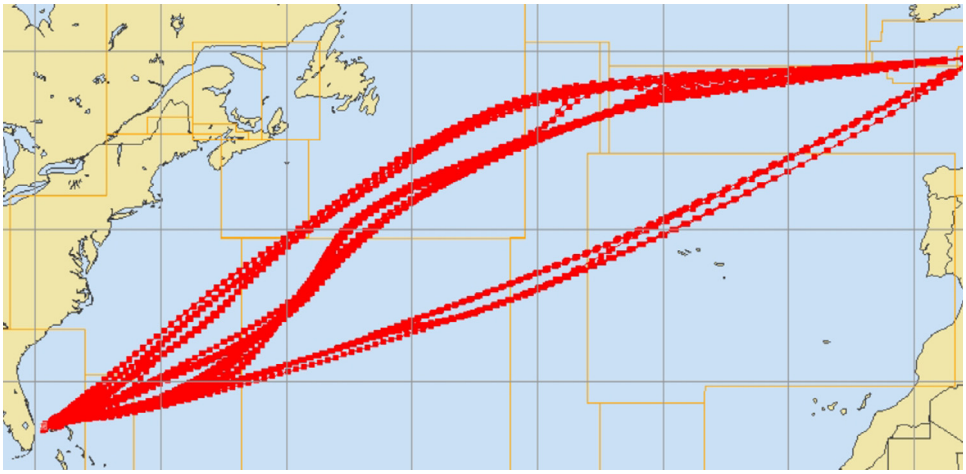

Fig. 11. Plymouth–Miami, departure on 27th September 2013 at 00:00 UTC, Pareto front (75 routes) obtained by MEWRA utilizing "regular Pareto dominance" (Case 0) in Scenario 2.

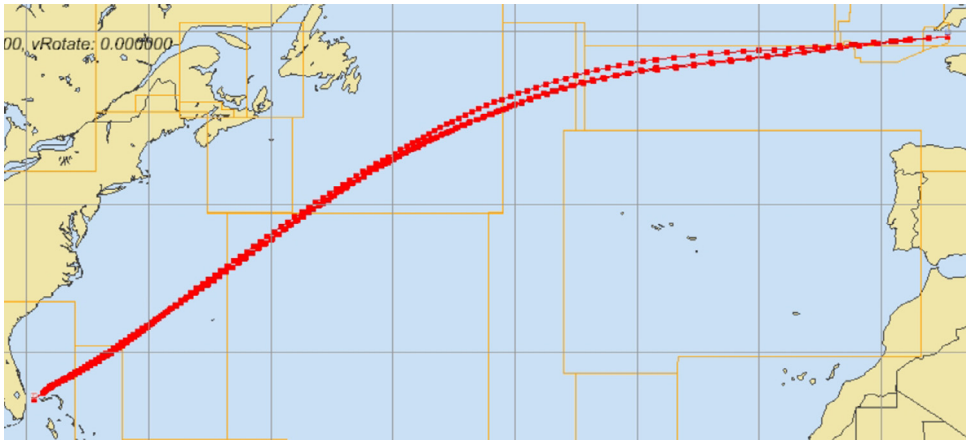

Fig. 12. Plymouth–Miami, departure on 27th September 2013 at 00:00 UTC, Pareto front (3 routes) obtained by MEWRA with weight intervals: passage time & fuel consumption: $w^{\min} = 0.5$ and $w^{\max} = 1.0$, safety of passage: $w^{\min} = 0.1$ and $w^{\max} = 0.5$ (Case 1) in Scenario 2.

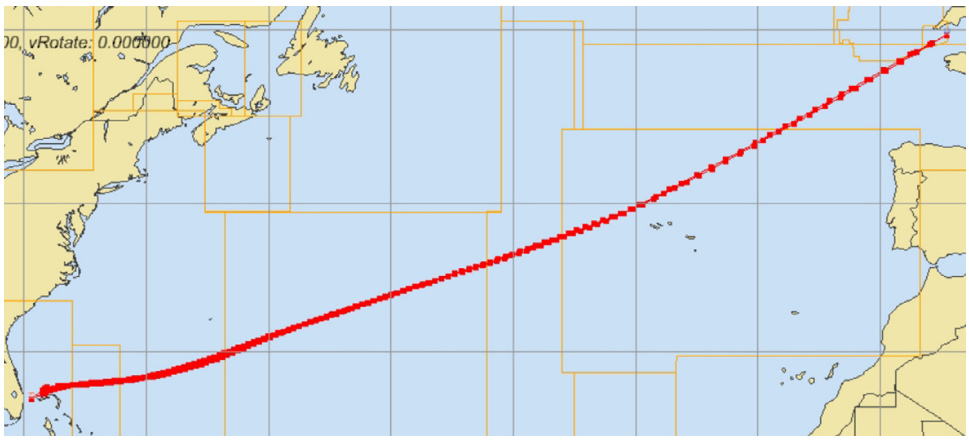

Fig. 13. Plymouth–Miami, departure on 27th September 2013 at 00:00 UTC, Pareto front (2 routes) obtained by MEWRA with weight intervals: passage time & fuel consumption: $w^{\min} = 0.1$ and $w^{\max} = 0.5$, safety of passage: $w^{\min} = 0.5$ and $w^{\max} = 1.0$ (Case 2) in Scenario 2.

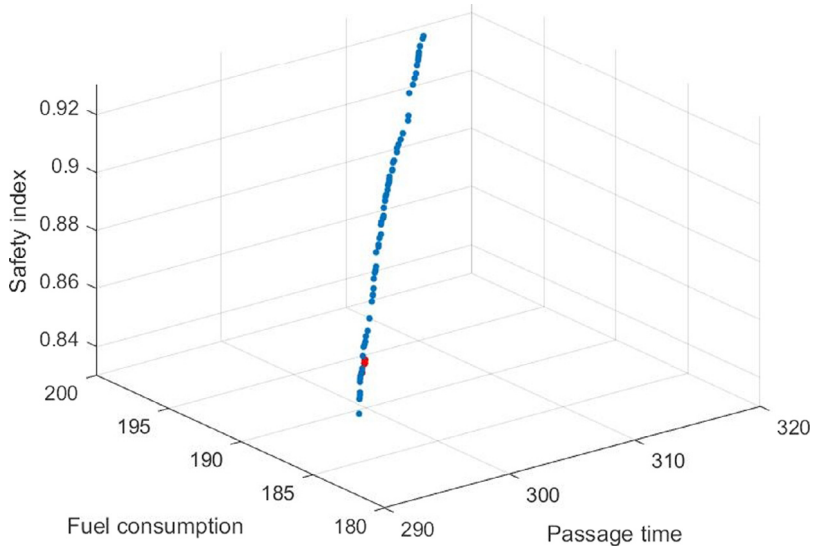

Fig. 14. Plymouth–Miami, departure on 27th September 2013 at 00:00 UTC, Pareto front (3 routes, red dots) in objective function space obtained by MEWRA with weight intervals: passage time & fuel consumption: $w^{\min} = 0.5$ and $w^{\max} = 1.0$, safety of passage: $w^{\min} = 0.1$ and $w^{\max} = 0.5$ (Case 1) with a reference Pareto front obtained by "regular domination" (blue dots) in Scenario 2.

fact that no proper estimations on route performance parameters such as passage time or fuel consumption can be made prior to obtaining exact solutions. Even though, a comparison test has been performed with assumption that DM is able to choose location of the RP based on Pareto front plot that is already available (as a result of "regular domination" applied to WR).

5.1. Configuration of r-dominance method

The authors of r-dominance [31] use the weighted Euclidean distance between a solution x and reference point g:

$$Dist(x,g) = \sqrt{\sum_{i=1}^{M} w_i \left(\frac{f_i(x) - f_i(g)}{f_i^{\max} - f_i^{\min}}\right)^2}, \quad w_i \in \langle 0,1\rangle, \sum_{i=1}^{M} w_i = 1, \tag{11}$$

where w_i are weights assigned to each objective and $f_i^{\max}, f_i^{\min}$ are upper and lower boundary of ith objective. As the method proposed in the current paper uses weight intervals $\langle w_i^{\min}, w_i^{\max}\rangle$also assigned to each objective, it has been decided that it would be best to set w_i in r-dominance method as middle points of those weight intervals and then re-scale w_i so that $\sum_{i=1}^{M} w_i = 1$.

$$w_i = \frac{u_i}{\sum_{i=1}^{M} u_i}, \tag{12}$$

where:

$$u_i = \frac{w_i^{\min} + w_i^{\max}}{2}. \tag{13}$$

Owing to this, both methods would reflect the same DM's preferences concerning objective's weights.

Another thing is that in r-dominance x dominates y if:

(1) x dominates y in the Pareto sense;

(2) x and y are Pareto-equivalent and $D(x,y,g) < -\delta$, where $\delta \in \langle 0,1\rangle$ and

$$D(x,y,g) = \frac{Dist(x,g) - Dist(y,g)}{Dist_{\max} - Dist_{\min}}, \tag{14}$$

where $Dist_{\max}, Dist_{\min}$ are maximal and minimal values of $Dist(z,g)$ over all solutions z within a generation and δ is the *non-r-dominance threshold.*

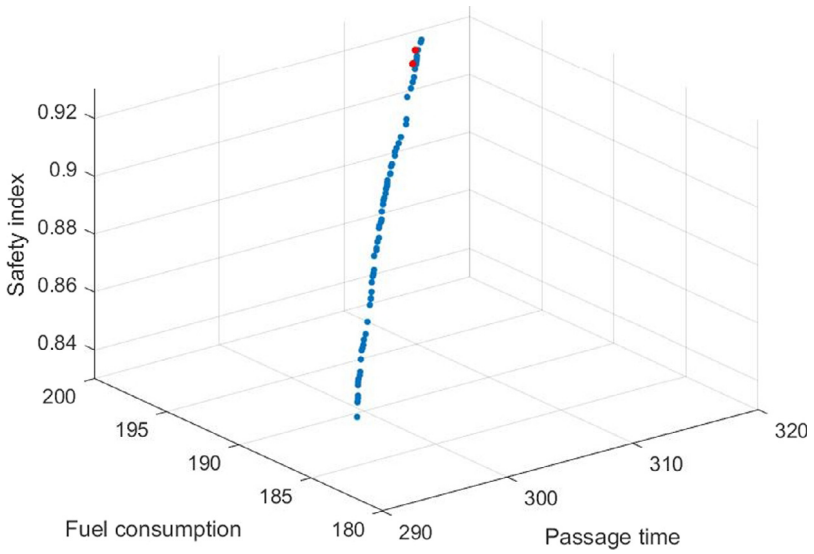

Fig. 15. Plymouth–Miami, departure on 27th September 2013 at 00:00 UTC, Pareto front (2 routes, red dots) in objective function space obtained by MEWRA with weight intervals: passage time & fuel consumption: $w^{\min} = 0.1$ and $w^{\max} = 0.5$, safety of passage: $w^{\min} = 0.5$ and $w^{\max} = 1.0$ (Case 2) with a reference Pareto front obtained by "regular domination" (blue dots) in Scenario 2.

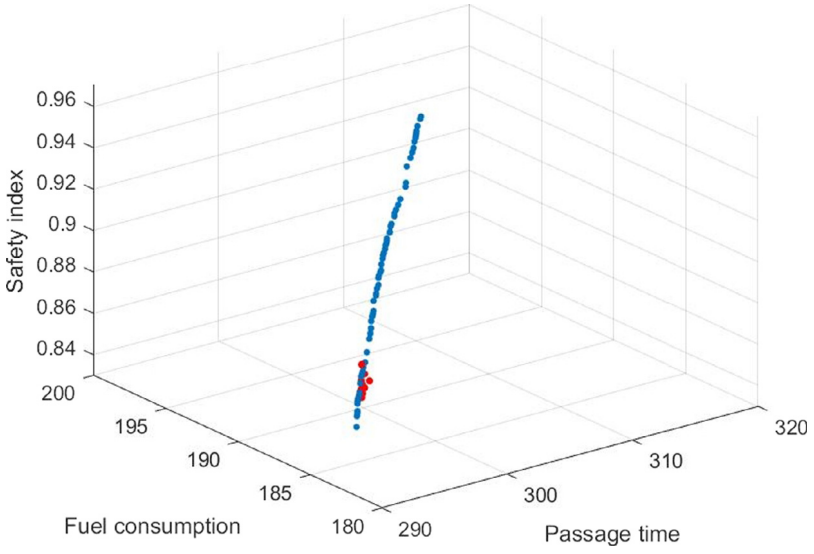

Fig. 16. Plymouth–Miami, departure on 27th September 2013 at 00:00 UTC, aggregated Pareto front (red dots) in objective function space obtained by MEWRA with weight intervals: passage time & fuel consumption: $w^{\min} = 0.5$ and $w^{\max} = 1.0$, safety of passage: $w^{\min} = 0.1$ and $w^{\max} = 0.5$ (Case 1) with a reference Pareto front obtained by "regular domination" (blue dots) in Scenario 2.

While in [31] δ can be any value from the $\langle 0, 1\rangle$ range, it is easy to observe that for $\delta = 0$ the dominance will nearly always occur either one direction or the other: a solution closer to reference point g will r-dominate the other. Analogically, for $\delta = 1$ the r-dominance will be reduced to regular Pareto dominance, because the second condition will never be satisfied ($D(x, y, g) < -1$ is never true).

It is important to note that exactly the same tendency occurs for widths of the weight intervals proposed in the current paper:

- the dominance always occurs for $w_i^{\min} = w_i^{\max}$ (interval's width equal to 0)
- the dominance is reduced to regular Pareto for $w_i^{\min} = 0$, $w_i^{\max} = 1$ (interval's width equal to 1).

In practice, in [31] it is recommended to decrease δ values linearly throughout the evolutionary process from 1 (for the first generation) to δ_user (for the last generation), where δ_user is specified by DM. Because of the above described tendencies of δ and interval widths, it was decided here to set δ_user as the weighted average of the intervals' widths:

$$\delta\_user = \sum_{i=1}^{M} w_i \left(w_i^{\max} - w_i^{\min}\right). \tag{15}$$

As a result, δ_user will be affected most by the widths of intervals assigned to those objectives, which were given largest weights by DM. Owing to this, despite completely different approaches used in both methods, they should apply roughly the same DM's preferences and the comparison results should be representative.

However, in the course of simulations it turned out that when δ_user were equal to average interval's width, relatively few r-dominance occurrences were registered. In practice, it had to be set to less than 0.5 to observe a significant reduction in the number of returned solutions. E.g. for $\delta_{user} = 0.33$the average

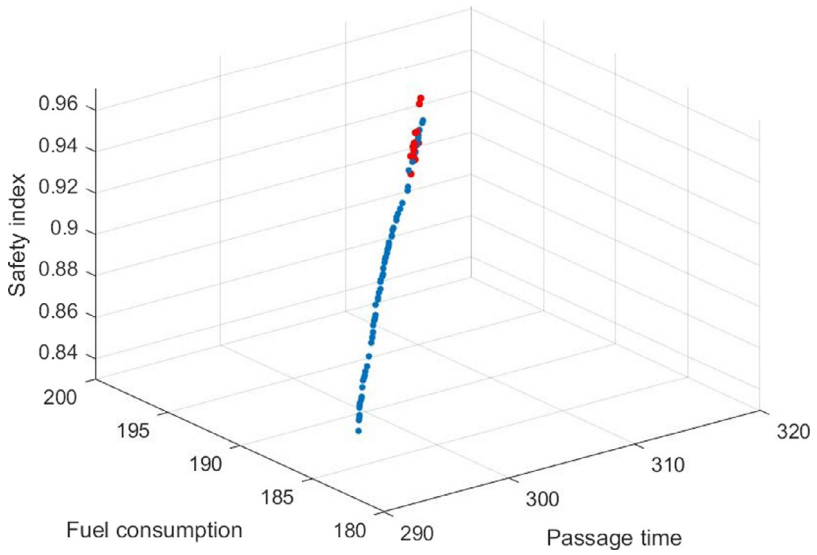

Fig. 17. Plymouth–Miami, departure on 27th September 2013 at 00:00 UTC, aggregated Pareto front (red dots) in objective function space obtained by MEWRA with weight intervals: passage time & fuel consumption: $w^{\min} = 0.1$ and $w^{\max} = 0.5$, safety of passage: $w^{\min} = 0.5$ and $w^{\max} = 1.0$ (Case 2) with a reference Pareto front obtained by "regular domination" (blue dots) in Scenario 2.

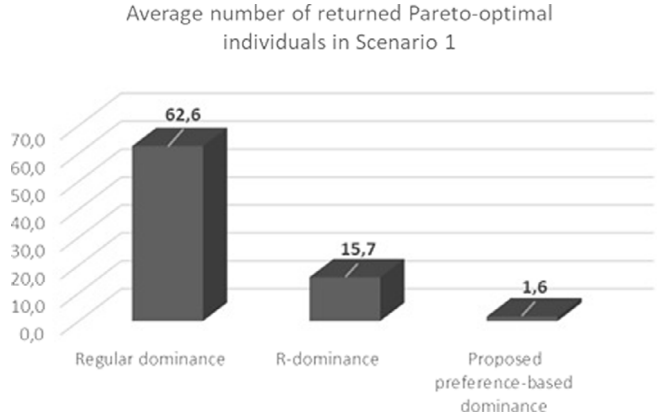

Fig. 18. Average number of returned Pareto-optimal individuals by various dominance approaches: regular, r- dominance and proposed preference-based dominance. DM's preferences are given by parameters: $w_i^{\min} = 0.33$, $w_i^{\max} = 0.66$ for all objectives, $\delta_{user} = 0.33$.

number of returned solutions was reduced from 63.5 (for regular Pareto dominance) to 15.67 (for r-dominance). At the same time the proposed preference-based method resulted in reduction to 1–2 returned solutions (1.6 on the average). Those differences are visualized in Fig. 18. Consequently, δ_{user} values of 0.33 and 0.2 have been chosen for the simulations presented in Section 5.2 because of their good performance, regardless of the fact that the weight intervals boundaries of the proposed approach were all set to $w_i^{\min} = 0.1$ and $w_i^{\max} = 0.9$.

5.2. Selecting reference points in r-dominance

The r-dominance method has been applied to MEWRA and tested on the input data from Scenario 1: voyage from Miami to Lisbon in February 2017. Results of our approach to dominance for the Scenario 1 have been presented earlier in the text in Section 4.1. Scenario 1 routes were sought by means of r-dominance applied to MEWRA for different locations of the reference point, based on Pareto front (from Fig. 8) obtained by "regular dominance" (without the modifications in Pareto-dominance proposed in this paper). The assumed six locations of RP point are presented in Fig. 19. Points #1 and #2 were chosen as end points (upper and lower) of the front, points #3 and #6 were located in the middle of the front, close by to the region of the red points found by our approach. In the contrary, points #4 and #5 were chosen in some distance from the front the way that point #4 is a dominated solution and point #5 is above the front level. Thus, the solution represented by point #5 is surely not attainable in practice.

5.3. Comparison results

In Figs. 20–25 Pareto fronts for Scenario 1 found by MEWRA are compared with r-dominance for $\delta = 0.2$ and reference points #1 - #6 (see Fig. 19 for the RP locations).

Fig. 20 presents results for the RP located in the lower end of Pareto front, which favours short passages with low fuel consumption at the cost of decreased safety index (routes more prone to ship stability-related issues). All the resulting r-dominance solutions (green dots) are inferior comparing to both the Pareto front found by regular domination (blue dots) and results obtained by the proposed preference-based approach (red dots). Namely, their passage time and fuel consumption values are higher for the same safety index values. The opposite situation is presented in Fig. 21, when the RP is located in the upper end of the front. This time routes assuring highest safety for the cost of a bit longer passage and higher fuel consumption are favoured. Here r-dominance results outperform elements of the (approximated) Pareto front with slightly higher safety indices for the same time and fuel values.

Two idealized cases (unlikely in practical WR applications) are presented in Figs. 22 and 25 (RP # 3 & #6), in which the RP is located centrally in the Pareto front. In both of these cases r-dominance results are very close to Pareto front and similar to the results returned by the proposed method.

In Figs. 23 and 24 RPs are located far outside the Pareto front. RP is underestimated for Fig. 23 and overestimated for Fig. 24. In both these cases r-dominance results are located away from the Pareto front. In case of the overestimated RP two individuals has been found by r-dominance that are slightly above the (approximated) Pareto front. However, all of the r-dominance results are highly inferior for underestimated RP (Fig. 23).

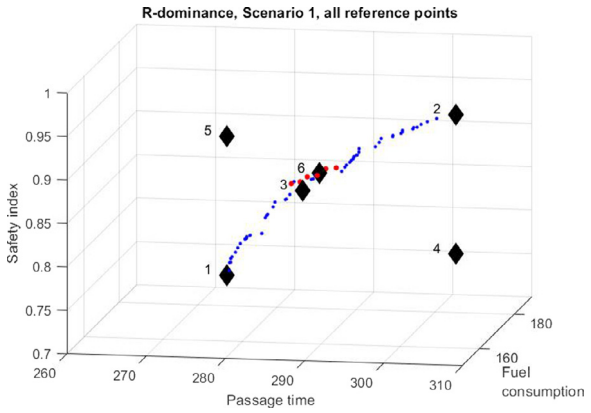

Fig. 19. Locations of six reference points (depicted by diamonds) in Scenario 1, together with (data taken from Fig. 8, with different viewing angle) reference Pareto front obtained by "regular domination" (blue dots) and MERWA solutions (6 routes, red dots) obtained with weight intervals $w^{\min} = 0.1$ and $w^{\max} = 0.9$ for each criterion (Case 1), Scenario 1, Miami–Lisbon, departure on 25th February 2017 at 00:00 UTC.

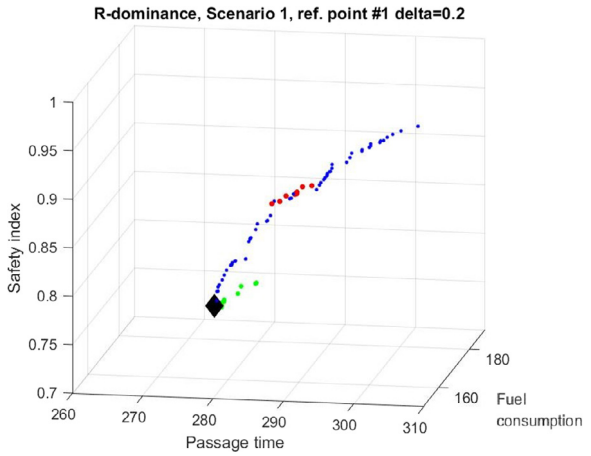

Fig. 20. Solutions (green dots) obtained by r-dominance with RP #1, $\delta = 0.2$ together with reference Pareto front (blue dots) and solutions by proposed preference-based dominance (red dots).

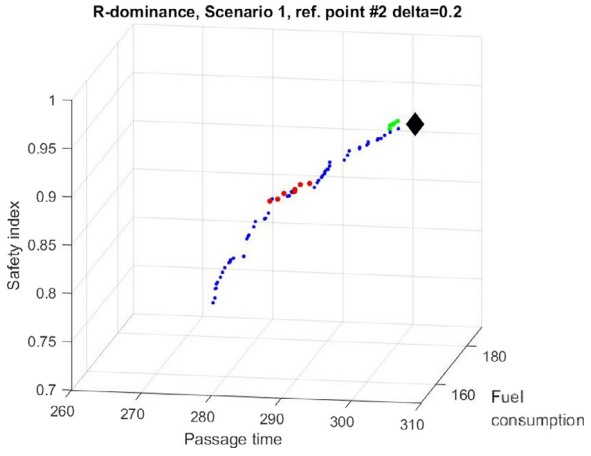

Fig. 21. Solutions (green dots) obtained by r-dominance with RP #2, $\delta = 0.2$ together with reference Pareto front (blue dots) and solutions by proposed preference-based dominance (red dots).

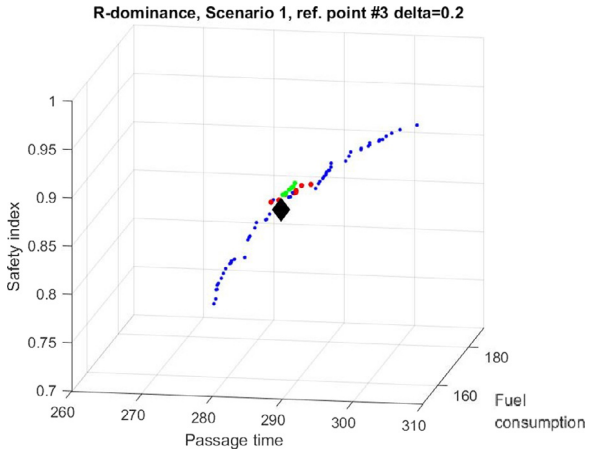

Fig. 22. Solutions (green dots) obtained by r-dominance with RP #3, $\delta = 0.2$ together with reference Pareto front (blue dots) and solutions by proposed preference-based dominance (red dots).

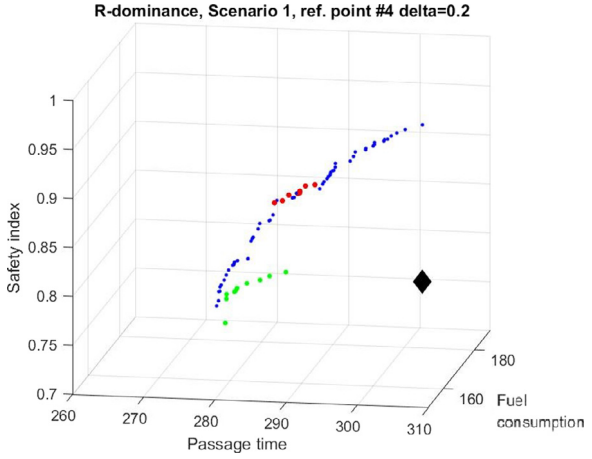

Fig. 23. Solutions (green dots) obtained by r-dominance with RP #4, $\delta = 0.2$ together with reference Pareto front (blue dots) and solutions by proposed preference-based dominance (red dots).

Figs. 26–31 present Pareto fronts for Scenario 1 found by MEWRA with r-dominance for the same reference points (RPs #1 - #6 as in Fig. 19) and $\delta = 0.33$. Similarly to the previous case (with $\delta = 0.2$) the RP has been set as following: to the lower end of Pareto front (Fig. 26), to the upper end of the front (Fig. 27), in the centre of the front (Figs. 28 and 31) and away from the front (Fig. 29 for underestimated point and Fig. 30 for overestimated one). As can be seen, similar tendencies of results can be observed. When compared to the Pareto fronts found by regular dominance, the r-dominance solutions are strongly inferior in case of an RP located in the upper end of a front (Fig. 26) or a heavily underestimated RP (Fig. 29). R-dominance scored much better for an RP in the upper end (Fig. 27) and an overestimated RP (Fig. 30). For both middle-located RPs (Figs. 28 and 31) r-dominance returns a set containing both superior and inferior solutions when compared to regular Pareto dominance. The inferior ones were usually far away from the approximated front, indicating that R-dominance is indeed prone to errors in case of unfortunate RP settings. In comparison, the proposed dominance method was always able to approximate with reasonable accuracy the part of the Pareto front, which DM specified by means of given weight intervals.

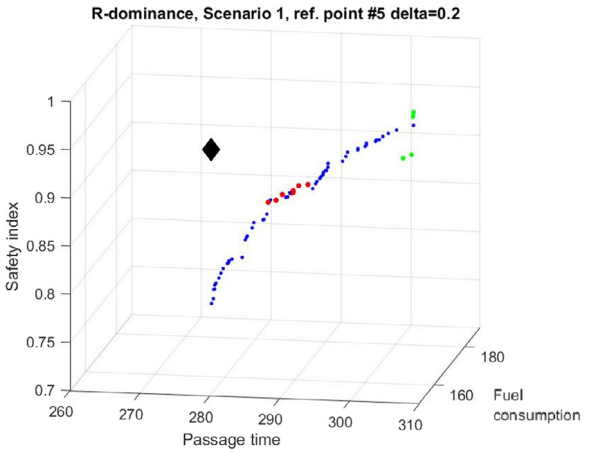

Fig. 24. Solutions (green dots) obtained by r-dominance with RP #5, $\delta = 0.2$ together with reference Pareto front (blue dots) and solutions by proposed preference-based dominance (red dots).

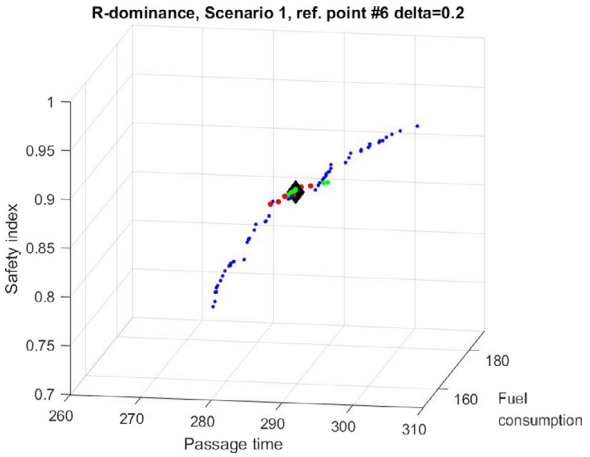

Fig. 25. Solutions (green dots) obtained by r-dominance with RP #6, $\delta = 0.2$ together with reference Pareto front (blue dots) and solutions by proposed preference-based dominance (red dots).

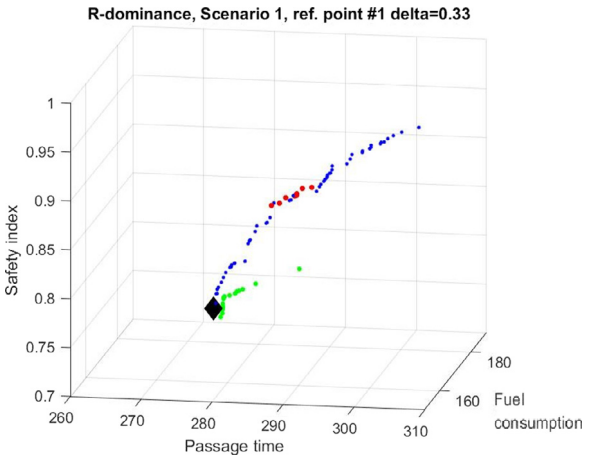

Fig. 26. Solutions (green dots) obtained by r-dominance with RP #1, $\delta = 0.33$ together with reference Pareto front (blue dots) and solutions by proposed preference-based dominance (red dots).

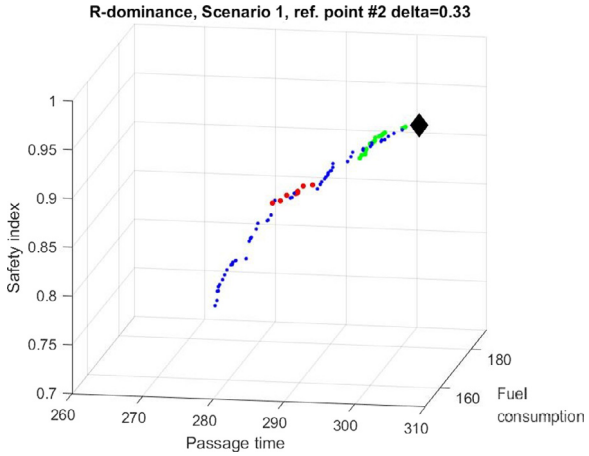

Fig. 27. Solutions (green dots) obtained by r-dominance with RP #2, $\delta = 0.33$ together with reference Pareto front (blue dots) and solutions by proposed preference-based dominance (red dots).

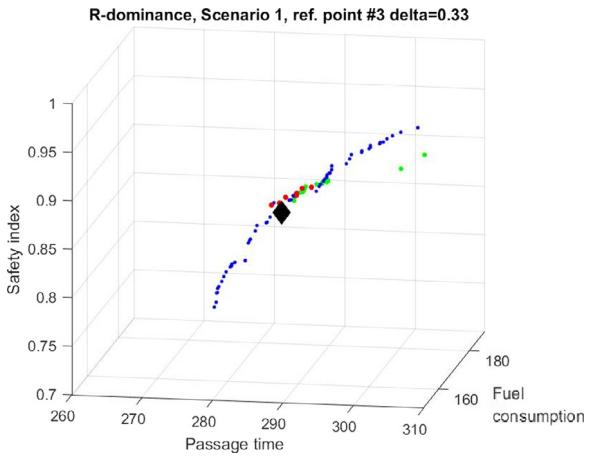

Fig. 28. Solutions (green dots) obtained by r-dominance with RP #3, $\delta = 0.33$ together with reference Pareto front (blue dots) and solutions by proposed preference-based dominance (red dots).

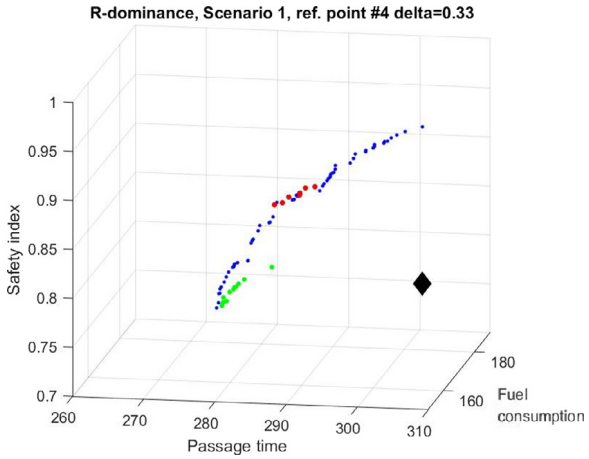

Fig. 29. Solutions (green dots) obtained by r-dominance with RP #4, $\delta = 0.33$ together with reference Pareto front (blue dots) and solutions by proposed preference-based dominance (red dots).

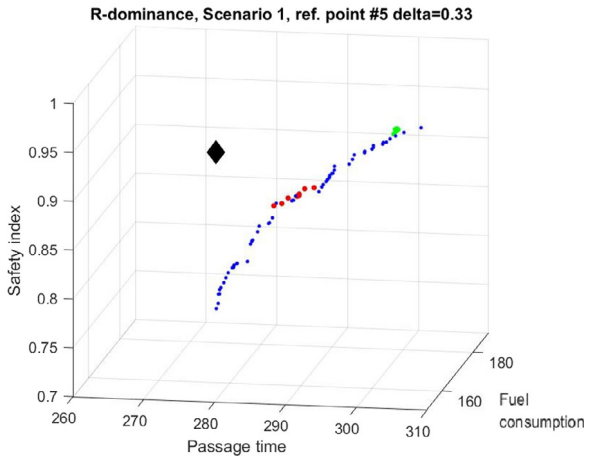

Fig. 30. Solutions (green dots) obtained by r-dominance with RP #5, $\delta = 0.33$ together with reference Pareto front (blue dots) and solutions by proposed preference-based dominance (red dots).

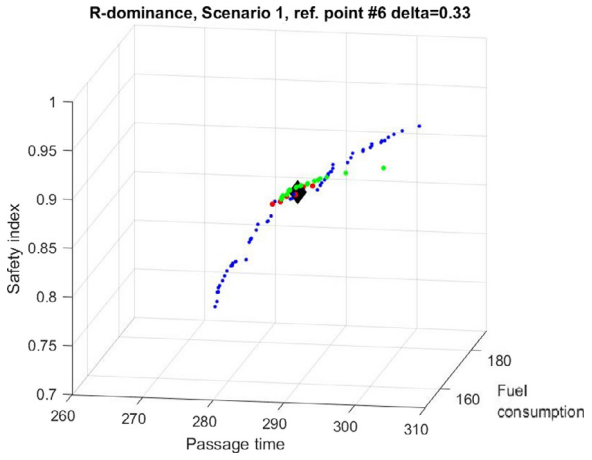

Fig. 31. Solutions (green dots) obtained by r-dominance with RP #6, $\delta = 0.33$ together with reference Pareto front (blue dots) and solutions by proposed preference-based dominance (red dots).

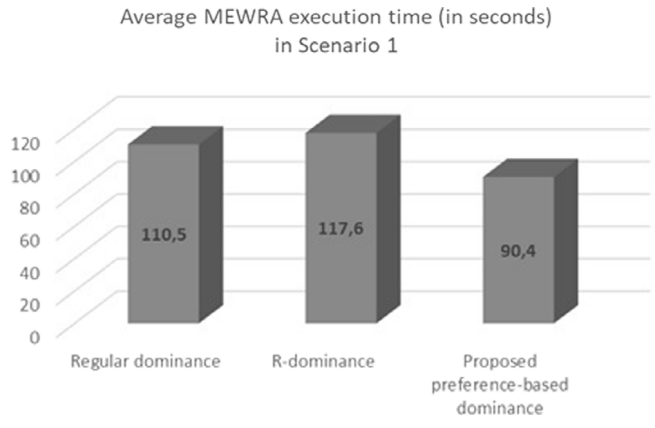

Fig. 32. Comparison of average MEWRA execution time (in seconds) in Scenario 1 with regular dominance, r-dominance and proposed preference-based dominance.

5.4. Comparison of MEWRA execution time with regular dominance, r-dominance and proposed preference-based dominance

Fig. 32 presents a comparison between execution time of the weather routing tool (MEWRA) with three possible approaches to Pareto dominance:

- regular dominance,
- r-dominance,
- the proposed dominance.

For all of them Scenario 1 has been run on a typical PC machine (Intel i7-6700 2.6 GHz, 16 GB RAM, Windows 10 x64). It is worth noting here that the majority of the computational time is spent on determining objective values, especially on checking vessel stability-related phenomena and bathymetric constraints. Those processes will not be shortened by including DM preferences, as long as the number of generations is constant (as it is in this section).

As can be seen in Fig. 32, application of the proposed dominance results in reduction of execution time by about 18% when compared to regular Pareto dominance. On the average (computed for the 6 RPs) r-dominance performs worse than the regular domination, however, as presented in Fig. 33, execution times for r-dominance differ significantly for various RP locations (RP#1–RP#6). Execution time depends greatly on safety index values of given RP: probably because safer routes are usually longer and their constraint check takes more time. The shortest execution time (even shorter than the average execution time for the proposed method) was achieved for RP#1 and RP#4, for which the assigned safety level is the lowest. However, in these cases obtained objective values were quite poor (inferior compared to the strict Pareto dominance and the proposed preference-based dominance: Figs. 20, 23, 26 and 29).

The most conclusive are results obtained by the proposed dominance and r-dominance for RP# 3 and RP#6. Both of these RPs are located in the central region of the Pareto front and their location corresponds well with the weight settings for the proposed method. When comparing RP#3 and RP #6 r-dominance time results with the proposed method, the latter is considerably faster.

5.5. Conclusions from the comparison with r-dominance

When comparing the proposed preference-based dominance with r-dominance, it might be concluded that the former is more stable in terms of both the quality of results (objective values) and execution times. R-dominance was occasionally able to outperform the proposed dominance (it achieved considerably better objective values), but it happened at the cost of significantly or even unacceptably worse results for some other cases. What is interesting, the poor r-dominance results occurred not only for unfortunate RP settings (which is understandable) but sometimes even for very reasonably located RPs (in the middle or bottom part of the Pareto front approximated by regular dominance). While it does not disqualify r-dominance as a preference-based method in EMO weather routing, it indicates that it requires either very careful and knowledge-based RP selection or repeated EMO runs with different RP settings. Finally, if both methods target the same part of the Pareto front, the proposed one returns results in a considerably shorter time.

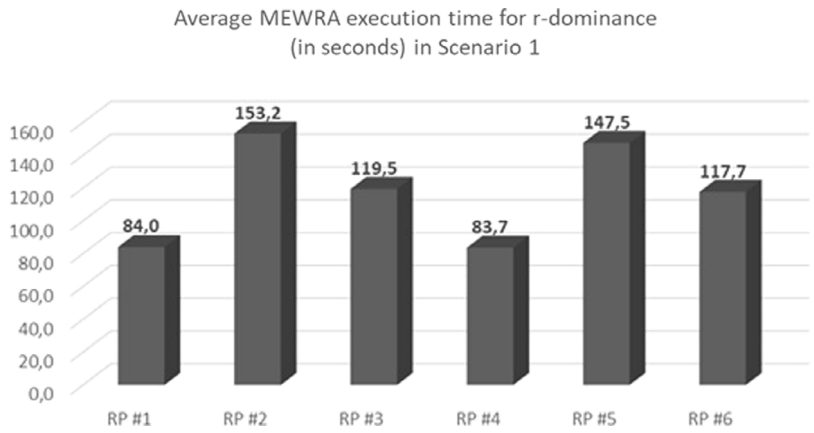

Fig. 33. Comparison of average MEWRA execution time (in seconds) in Scenario 1 with r-dominance and six different locations of the reference points (RP#1–RP#6) as defined previously in Fig. 19.

6. Summary

Finding a balance between economy and safety in ship weather routing (WR) obviously is one of the key ideas driving the IT supported maritime industry. When the ship routing problem is solved from the multi-objective Pareto perspective one gets as a result a set of numerous non-dominated routes. Commonly, a MCDM ranking method can be applied in the post-optimization phase to select a single route that may be recommended to the navigator. However, a well-grounded preference-based limitation of the problem's objective space may result in obtaining the proper economy & safety balance much easier and considerably faster. This is exactly what the paper offers: it introduces weight intervals to the preference-based EMO and applies it to the weather routing optimization problem. As a result the EMO weather routing method is able to target a selected part of the true Pareto front and approximate it with reasonable accuracy in a shorter time. From the navigator's or a ship-owner's point of view this is a significant advantage as they can enter their preferences and simplify the final choice by limiting the returned set routes. The paper makes an effort to meet user's needs towards obtaining the balance determined by DM's preferences. As it is shown in the provided examples the solution is both easily configurable and robust.

The proposed method has been compared with one of the most successful reference point (RP) approaches to incorporating DM's preferences — r-dominance. As it turned out, the proposed approach can score better than r-dominance, because the latter method's performance is heavily affected by the choice of RP coordinates, which may be hard to specify in case of WR. The above applies to the quality of results as well as execution times of the compared approaches. It must be emphasized here that the authors do not claim that the proposed approach is in general competitive to other preference-based methods. But it certainly has significant advantages in case of WR problem and might also be an interesting choice in similar applications, where environment dynamics make it impossible to rely on past data and provide reasonable RPs. Moreover, typically for trade-off approach, the proposed method is context-free as the input weight intervals reflect only DM's actual preferences without involving DM's assessment of what is feasible in a particular case.

Future plans to develop the research on preference-based EMO with weight intervals applied to WR problem include changes in the main optimization algorithm as well as the weather data sources and handling those data by the method. As for the EMO algorithm, SPEA 2 will be replaced with MOEA/D, due to the latter's better coverage of a Pareto front. In terms of weather data, the current model will be replaced by GFS (for wind and waves), RTOFS (for ocean currents) and GWES (for ensemble forecasts of significant wave height) models. Following this, further work will aim at developing a prototype of an on-board decision support system for route planning. It is expected that it should be possible within the scope of the ROUTING project within next 18 months.

Declaration of competing interest

No author associated with this paper has disclosed any potential or pertinent conflicts which may be perceived to have impending conflict with this work. For full disclosure statements refer to https://doi.org/10.1016/j.asoc.2019.105742.

Acknowledgements

This research was supported by The National Centre for Research and Development in Poland under grant on ROUTING research project (MARTERA-1/ROUTING/3/2018) in ERA-NET CO-FUND MarTERA-1 programme (2018–2021).

Appendix A. Wind conditions forecasted for the voyages in scenario 1 & scenario 2

This appendix presents wind forecast (speed and direction) from NOAA Wave Watch III model obtained for departure time for the considered scenarios, namely:

1. Scenario 1: voyage Miami–Lisbon on 25th February 2017 at 00:00 UTC (see Fig. A.1).
2. Scenario 2: voyage Plymouth–Miami on 27th September 2013 at 00:00 UTC (see Fig. A.2).

The following subsections cover each of the scenario separately. Apart from figures presenting wind forecasts there are also available animation files in supplementary data.

Appendix B. Supplementary data

Supplementary material related to this article can be found online at https://doi.org/10.1016/j.asoc.2019.105742.

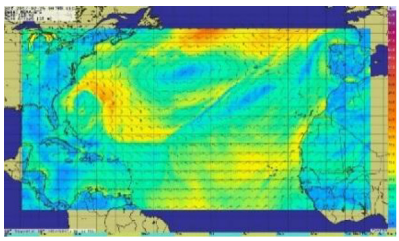

Figure A 0-1 2017.02.25 00:00 UTC

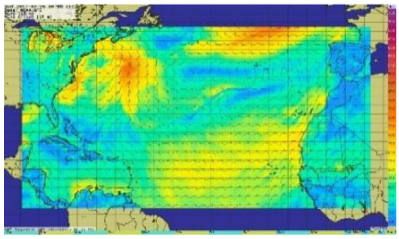

Figure A 0-2 2017.02.26 00:00 UTC

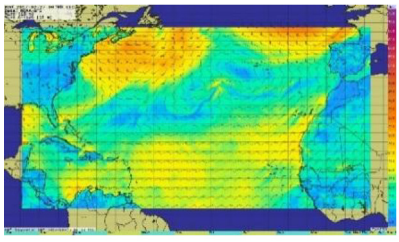

Figure A 0-3 2017.02.27 00:00 UTC

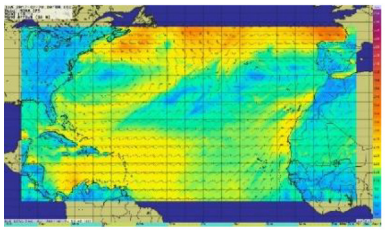

Figure A 0-4 2017.02.28 00:00 UTC

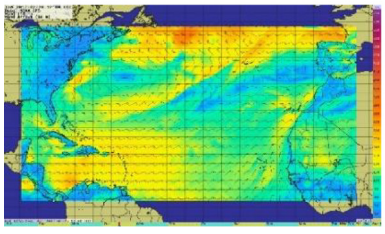

Figure A 0-5 2017.03.01 00:00 UTC

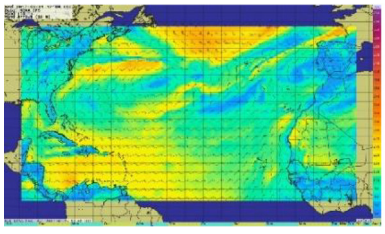

Figure A 0-6 2017.03.02 00:00 UTC

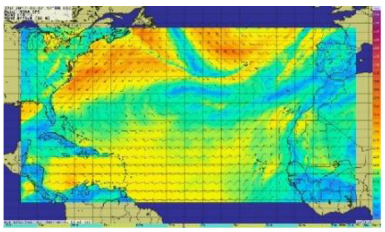

Figure A 0-7 2017.03.03 00:00 UTC

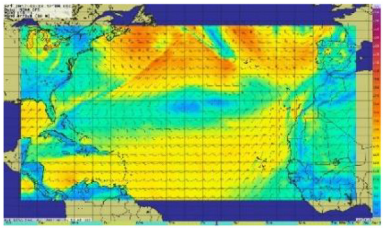

Figure A 0-8 2017.03.04 00:00 UTC

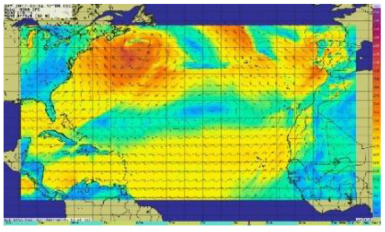

Figure A 0-9 2017.03.05 00:00 UTC

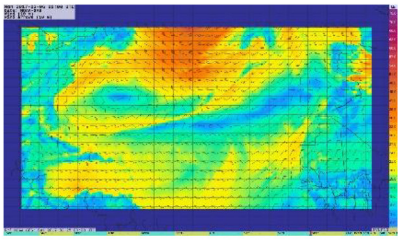

Figure A 0-10 2017.03.06 00:00 UTC

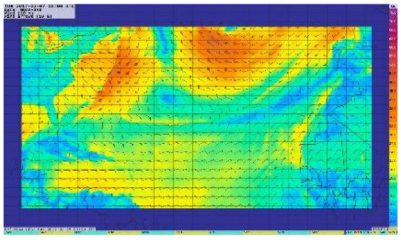

Figure A 0-11 2017.03.07 00:00 UTC

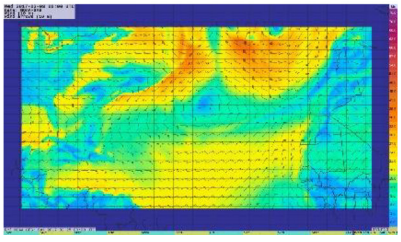

Figure A 0-12 2017.03.08 00:00 UTC

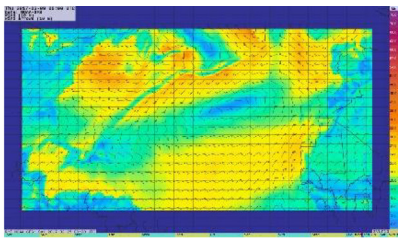

Figure A 0-13 2017.03.09 00:00 UTC

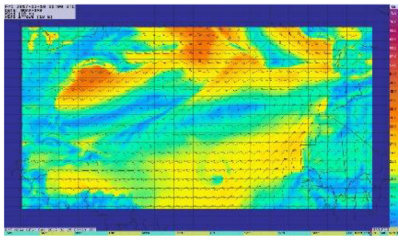

Figure A 0-14 2017.03.10 00:00 UTC

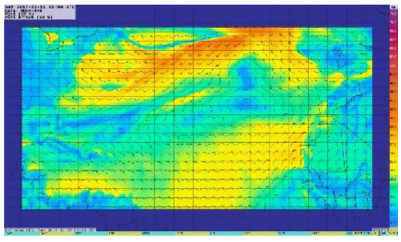

Figure A 0-15 2017.03.11 00:00 UTC

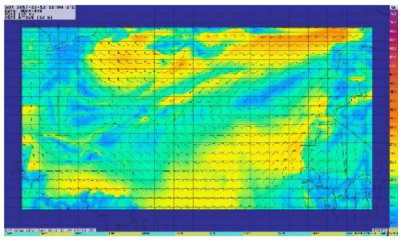

Figure A 0-16 2017.03.12 00:00 UTC

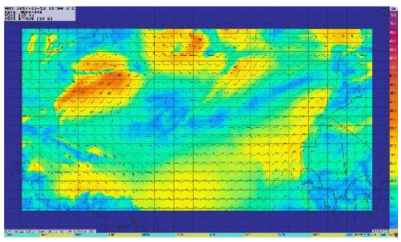

Figure A 0-17 2017.03.13 00:00 UTC

Fig. A.1. Wind conditions (speed & direction) forecasted for the voyage in Scenario 1: Miami–Lisbon, departure on 25th February 2017 at 00:00 UTC.

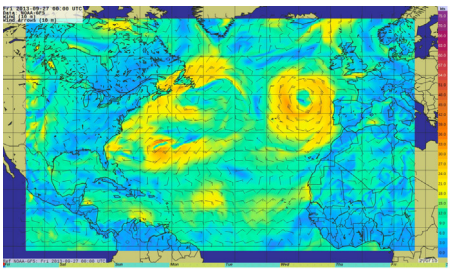

Figure A 2-1 2013.09.27 00:00 UTC

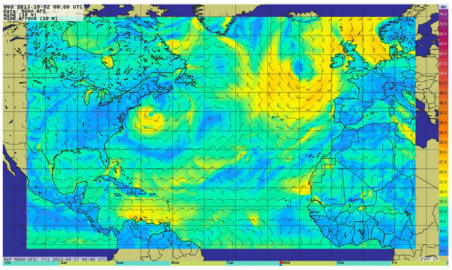

Figure A 2-6 2013.10.02 00:00 UTC

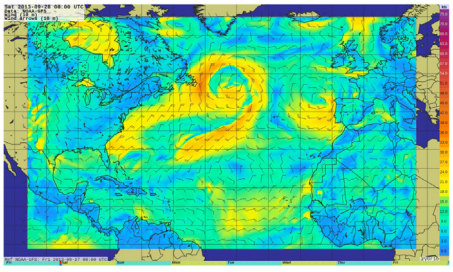

Figure A 2-2 2013.09.28 00:00 UTC

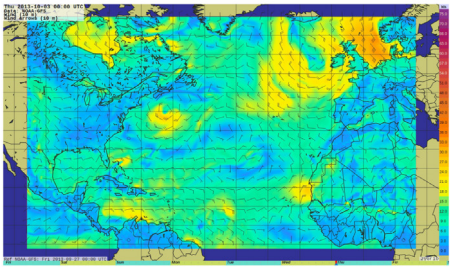

Figure A 2-7 2013.10.03 00:00 UTC

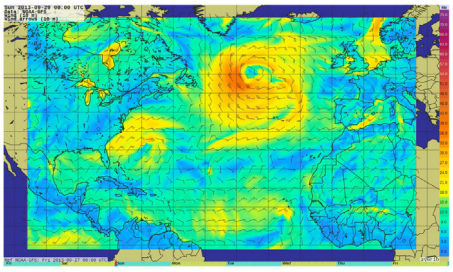

Figure A 2-3 2013.09.29 00:00 UTC

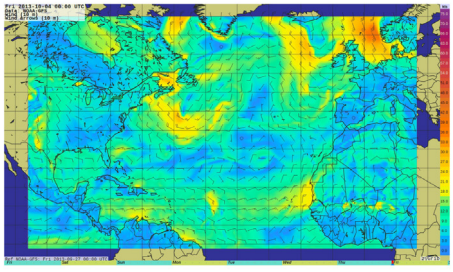

Figure A 2-8 2013.10.04 00:00 UTC

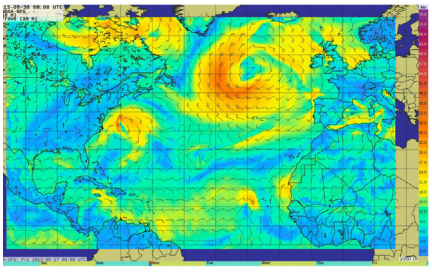

Figure A 2-4 2013.09.30 00:00 UTC

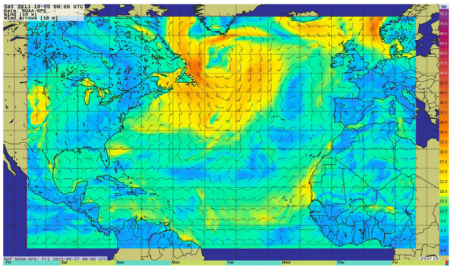

Figure A 2-9 2013.10.05 00:00 UTC

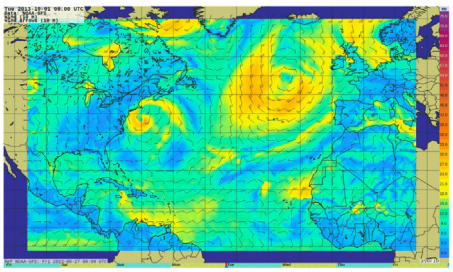

Figure A 2-5 2013.10.01 00:00 UTC

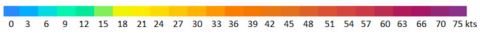

Figure A 2-10 Wind speed value (knots) legend

Fig. A.2. Wind conditions (speed & direction) forecasted for the voyage in Scenario 2: Plymouth–Miami, departure on 27th September 2013 at 00:00 UTC.

References

[1] M.-C. Tsou, H.-C. Cheng, An ant colony algorithm for efficient ship routing, Polish Marit. Res. 20 (2013) 28–38, http://dx.doi.org/10.2478/pomr-2013-0032.

[2] S. Chaudhuri, K. Deb, An interactive evolutionary multi-objective optimization and decision making procedure, Appl. Soft Comput. J. 10 (2010) 496–511, http://dx.doi.org/10.1016/j.asoc.2009.08.019.

[3] H. Lu, R. Zhou, Z. Fei, J. Shi, A multi-objective evolutionary algorithm based on Pareto prediction for automatic test task scheduling problems, Appl. Soft Comput. 66 (2018) 394–412, http://dx.doi.org/10.1016/J.ASOC.2018.02.050.

[4] P. Fattahi, V. Hajipour, A. Nobari, A bi-objective continuous review inventory control model: Pareto-based meta-heuristic algorithms, Appl. Soft Comput. 32 (2015) 211–223, http://dx.doi.org/10.1016/J.ASOC.2015.02.044.

[5] B. Min, C. Park, I. Jang, J.M. Kang, S. Chung, Development of Pareto-based evolutionary model integrated with dynamic goal programming and successive linear objective reduction, Appl. Soft Comput. 35 (2015) 75–112, http://dx.doi.org/10.1016/J.ASOC.2015.06.007.

[6] R. Szlapczynski, P. Krata, Determining and visualizing safe motion parameters of a ship navigating in severe weather conditions, Ocean Eng. 158 (2018) http://dx.doi.org/10.1016/j.oceaneng.2018.03.092.

[7] A.C. Bukhari, I. Tusseyeva, B.G. Lee, Y.G. Kim, An intelligent real-time multi-vessel collision risk assessment system from VTS view point based on fuzzy inference system, Expert Syst. Appl. 40 (2013) 1220–1230, http://dx.doi.org/10.1016/j.eswa.2012.08.016.

[8] J. Lisowski, Game control methods in avoidance of ships collisions, Polish Marit. Res. 19 (2012) 3–10, http://dx.doi.org/10.2478/v10012-012-0016-4.

[9] A. Lazarowska, A new deterministic approach in a decision support system for ship's, Expert Syst. Appl. (2016) 1–10, http://dx.doi.org/10.1016/j.eswa.2016.11.005.

[10] R.W. James, Application of Wave Forecasts To Marine Navigation, 1957.

[11] H. Hagiwara, J.A. Spaans, Practical weather routing of sail-assisted motor vessels, J. Navig. 40 (1987) 96–119, http://dx.doi.org/10.1017/S0373463300000333.

[12] R.H. Motte, S. Calvert, On the selection of discrete grid systems for on-board micro-based weather routeing, J. Navig. 43 (1990) 104–117, http://dx.doi.org/10.1017/S0373463300013849.

[13] C. de Wit, Proposal for low cost ocean weather routeing, J. Navig. 43 (1990) 428–439, http://dx.doi.org/10.1017/S0373463300014053.

[14] S. Wei, P. Zhou, Development of a 3D dynamic programming method for weather routing, Int. J. Mar. Navig. Saf. Sea Transp. 6 (2012) 79–85.

[15] Y.-C. Chang, R.-S. Tseng, G.-Y. Chen, P.C. Chu, Y.-T. Shen, Ship routing utilizing strong ocean currents, J. Navig. 66 (2013) 825–835, http://dx.doi.org/10.1017/S0373463313000441.

[16] S.J. Bijlsma, Minimal time route computation for ships with pre-specified voyage fuel consumption, J. Navig. 61 (2008) 723–733, http://dx.doi.org/10.1017/S037346330800492X.

[17] G. Mannarini, G. Coppini, P. Oddo, N. Pinardi, A prototype of ship routing decision support system for an operational oceanographic service, TransNav - Int. J. Mar. Navig. Saf. Sea Transp. 7 (2013) 53–59, http://dx.doi.org/10.12716/1001.07.01.06.

[18] G. Mannarini, N. Pinardi, G. Coppini, P. Oddo, A. Iafrati, I. Nazionale, V.D. Creti, VISIR-I: small vessels – least-time nautical routes using wave forecasts, Geosci. Model Dev. 9 (2016) 1597–1625, http://dx.doi.org/10.5194/gmd-9-1597-2016.

[19] M. Zyczkowski, R. Szłapczyński, Multi-objective weather routing of sailing vessels, Polish Marit. Res. 24 (2017) http://dx.doi.org/10.1515/pomr-2017-0130.

[20] M. Zyczkowski, P. Krata, R. Szłapczyński, Multi-objective weather routing of sailboats considering wave resistance, Polish Marit. Res. 25 (2018) 4–12, http://dx.doi.org/10.2478/pomr-2018-0001.

[21] M.C. Tsou, Integration of a geographic information system and evolutionary computation for automatic routing in coastal navigation, J. Navig. 63 (2010) 323–341, http://dx.doi.org/10.1017/S0373463309990385.

[22] J. Szlapczynska, Multiobjective approach to weather routing, TransNav - Int. J. Mar. Navig. Saf. Sea Transp. 1 (2007) 273–278.

[23] S. Marie, E. Courteille, Multi-objective optimization of motor vessel route, TransNav - Int. J. Mar. Navig. Saf. Sea Transp. 3 (2009) 133–141.

[24] J. Hinnenthal, G. Clauss, Robust Pareto-optimum routing of ships utilising deterministic and ensemble weather forecasts, Ships Offshore Struct. 5 (2010) 105–114, http://dx.doi.org/10.1080/17445300903210988.

[25] R. Vettor, C. Guedes Soares, A Ship Weather Routing Toll to Face the Challenges of an Evolving Maritime Trade, 2015.

[26] R. Vettor, C. Guedes Soares, Development of a ship weather routing system, Ocean Eng. 123 (2016) 1–14, http://dx.doi.org/10.1016/j.oceaneng.2016.06.035.

[27] S. Bechikh, M. Kessentini, L. Ben Said, K. Ghédira, Preference incorporation in evolutionary multiobjective optimization: A survey of the state-of-the-art, Adv. Comput. 98 (2015) 141–207, http://dx.doi.org/10.1016/bs.adcom.2015.03.001.

[28] K. Sindhya, K. Miettinen, K. Deb, A hybrid framework for evolutionary multi-objective optimization, IEEE Trans. Evol. Comput. 17 (2013) 495–511, http://dx.doi.org/10.1109/TEVC.2012.2204403.

[29] K. Deb, H. Jain, An evolutionary many-objective optimization algorithm using reference-point-based nondominated sorting approach, Part I: Solving problems with box constraints, IEEE Trans. Evol. Comput. 18 (2014) 577–601, http://dx.doi.org/10.1109/TEVC.2013.2281535.

[30] H. Ishibuchi, R. Imada, Y. Setoguchi, Y. Nojima, Reference point specification in inverted generational distance for triangular linear Pareto front, IEEE Trans. Evol. Comput. 22 (2018) 961–975, http://dx.doi.org/10.1109/TEVC.2017.2776226.

[31] L. Ben Said, S. Bechikh, K. Ghedira, The r-dominance: A new dominance relation for interactive evolutionary multicriteria decision making, IEEE Trans. Evol. Comput. 14 (2010) 801–818, http://dx.doi.org/10.1109/TEVC.2010.2041060.

[32] A.L. Jaimes, A.A. Montaño, C.A.C. Coello, Preference incorporation to solve many-objective airfoil design problems, in: 2011 IEEE Congr. Evol. Comput, CEC 2011, 2011, pp. 1605–1612, http://dx.doi.org/10.1109/CEC.2011.5949807.

[33] K. Miettinen, F. Ruiz, A.P. Wierzbicki, Introduction to multiobjective optimization: Interactive approaches, in: J. Branke, K. Deb, K. Miettinen, R. Słowiński (Eds.), Multiobjective Optim. Interact. Evol. Approaches, Springer Berlin Heidelberg, Berlin, Heidelberg, 2008, pp. 27–57, http://dx.doi.org/10.1007/978-3-540-88908-3_2.

[34] E. Filatovas, A. Lančinskas, O. Kurasova, J. Žilinskas, A preference-based multi-objective evolutionary algorithm R-NSGA-II with stochastic local search, Cent. Eur. J. Oper. Res. 25 (2017) 859–878, http://dx.doi.org/10.1007/s10100-016-0443-x.

[35] K. Deb, A. Kumar, Light beam search based multi-objective optimization using evolutionary algorithms, in: 2007 IEEE Congr. Evol. Comput. CEC 2007, 2007, pp. 2125–2132, http://dx.doi.org/10.1109/CEC.2007.4424735.

[36] H. Trautmann, T. Wagner, D. Brockhoff, R2-EMOA: Focused multiobjective search using R2-indicator-based selection, in: G. Nicosia, P. Pardalos (Eds.), Learn. Intell. Optim, Springer Berlin Heidelberg, Berlin, Heidelberg, 2013, pp. 70–74.

[37] G. Rudolph, O. Schütze, C. Grimme, H. Trautmann, An aspiration set EMOA based on averaged hausdorff distances, in: P.M. Pardalos, M.G.C. Resende, C. Vogiatzis, J.L Walteros (Eds.), Learn. Intell. Optim., Springer International Publishing, Cham, 2014, pp. 153–156.

[38] E. Zitzler, D. Brockhoff, L. Thiele, The hypervolume indicator revisited: On the design of Pareto-compliant indicators via weighted integration, in: S. Obayashi, K. Deb, C. Poloni, T. Hiroyasu, T. Murata (Eds.), Evol. Multi-Criterion Optim., Springer Berlin Heidelberg, Berlin, Heidelberg, 2007, pp. 862–876.

[39] M.T.M. Emmerich, A.H. Deutz, I. Yevseyeva, On Reference Point Free Weighted Hypervolume Indicators Based on Desirability Functions and their Probabilistic Interpretation, Elsevier B.V., 2014, http://dx.doi.org/10.1016/j.protcy.2014.10.001.

[40] D. Brockhoff, Y. Hamadi, S. Kaci, Using comparative preference statements in hypervolume-based interactive multiobjective optimization to cite this version: Using comparative preference statements in hypervolume-based interactive multiobjective, Learn. Intell. Optim. (2014).

[41] J. Branke, S. Corrente, S. Greco, R. Słowiński, P. Zielniewicz, Using choquet integral as preference model in interactive evolutionary multiobjective optimization, European J. Oper. Res. 250 (2016) 884–901, http://dx.doi.org/10.1016/j.ejor.2015.10.027.

[42] E. Fernandez, E. Lopez, F. Lopez, C.A. Coello Coello, Increasing selective pressure towards the best compromise in evolutionary multiobjective optimization: The extended NOSGA method, Inf. Sci. (Ny). 181 (2011) 44–56, http://dx.doi.org/10.1016/j.ins.2010.09.007.

[43] E. Oliveira, C.H. Antunes, Á. Gomes, A comparative study of different approaches using an outranking relation in a multi-objective evolutionary algorithm, Comput. Oper. Res. 40 (2013) 1602–1615, http://dx.doi.org/10.1016/j.cor.2011.09.023.

[44] S. Bechikh, L. Ben Said, K. Ghédira, Searching for knee regions of the Pareto front using mobile reference points, Soft Comput. 15 (2011) 1807–1823, http://dx.doi.org/10.1007/s00500-011-0694-3.

[45] J. Branke, T. Kaußler, H. Schmeck, Guidance in evolutionary multi-objective optimization, Adv. Eng. Softw. 32 (2001) 499–507, http://dx.doi.org/10.1016/S0965-9978(00)00110-1.

[46] D. Cvetković, I.C. Parmee, Preferences and their application in evolutionary multiobjective optimization, IEEE Trans. Evol. Comput. 6 (2002) 42–57, http://dx.doi.org/10.1109/4235.985691.

[47] P.K. Shukla, C. Hirsch, H. Schmeck, A framework for incorporating trade-off information using multi-objective evolutionary algorithms, in: R. Schaefer, C. Cotta, J. Kołodziej, G. Rudolph (Eds.), Parallel Probl. Solving from Nature, PPSN XI, Springer Berlin Heidelberg, Berlin, Heidelberg, 2010, pp. 131–140.

[48] Y. Jin, B. Sendhoff, Incorporation of fuzzy preferences into evolutionary multiobjective optimisation, in: Proc. Genet. Evol. Comput. Conf. GECCO, 2002, p. 683.

[49] J. Szlapczynska, Multi-objective weather routing with customised criteria and constraints, J. Navig. 68 (2015) http://dx.doi.org/10.1017/S0373463314000691.
[50] P. Krata, J. Szlapczynska, Ship weather routing optimization with dynamic constraints based on reliable synchronous roll prediction, Ocean Eng. 150 (2018) 124–137, http://dx.doi.org/10.1016/j.oceaneng.2017.12.049.
[51] P. Krata, J. Szlapczynska, Weather hazard avoidance in modeling safety of motor-driven ship for multicriteria weather routing, in: Methods Algorithms Navig., 2012, http://dx.doi.org/10.1201/b11344-27.
[52] E. Zitzler, M. Laumanns, L. Thiele, SPEA2: Improving the strength Pareto evolutionary algorithm, Evol. Methods Des. Optim. Control with Appl. Ind. Probl. (2001) 95–100, http://dx.doi.org/10.1.1.28.7571.